Republic of Iraq
Ministry of Higher Education and Scientific Research
University of Babylon

College of Engineering

Properties and Mechanism of Ceramic(Al_2O_3) / Metal(Cu) Bonding

A Thesis

Submitted to College of Engineering / University of Babylon

in Partial Fulfillment of the Requirements for the Degree of Ph.D.

in Materials Engineering

By

Ahmed Ouda Jasim Al-Rubaii

Supervisor

Prof.Dr. Abd.Al- Wahed K.Rajih **Dr.Fadhel Abbas Hashim**

August, ٢٠٠٧

جمهورية العراق
وزارة التعليم العالي والبحث العلمي
جامعة بابل
كلية الهندسة

خواص وآلية ترابط السيراميك(الألومينا) / المعدن(النحاس)

رسالة مقدمة إلى كلية الهندسة
في جامعة بابل وهي جزء من متطلبات نيل شهادة الدكتوراه
في هندسة المواد

من قبل
أحمد عوده جاسم الربيعي

ا.د.عبد الواحد كاظم راجح ا.م.د.فاضل عباس هاشم

١٤٢٨ هـ ٢٠٠٧م

Republic of Iraq
Ministry of Higher Education and Scientific Research
University of Babylon

College of Engineering

Properties and Mechanism of Ceramic(Al_2O_3) / Metal(Cu) Bonding

A Thesis

Submitted to College of Engineering / University of Babylon

in Partial Fulfillment of the Requirements for the Degree of Ph.D. in Materials Engineering

By

Ahmed Ouda Jasim Al-Rubaii

August, ٢٠٠٧

Acknowledgements

I would like to express my gratitude to my supervisors, prof.Dr.Abdual-Wahid Kadhim Rajih and Dr.Fadhel Abbas Hashem who have been guidance, advice and enthusiastic encouragement throughout this investigation.

I am grateful to the department of material, college of engineering, University of Babylon especially to the head of the department Dr.Najim Abdual-Amear who have been very encourages and supportive of this work.

I would like to thank the staff of the workshop ,materials lab. in Babylon University.Sepecial thanks are offered to Mr. Jameel Abdual-Hour .

Finally, words not enough to thank my family encouragement ; my wife, doughters,sons for their support, patience and self-sacrifice through all these years. A lot of appreciation I expressed to my ;sisters and my brothers for the continuous encouragement

Supervisors Certificate

We certify that this thesis entitled (*Properties and Mechanism of Ceramic(Al_2O_3)/Metal(Cu) Bonding*)prepared by Ahmed Ouda Jasim was carried out under my supervision at the Department of Material Engineering, College of Engineering, Babylon University in partial fulfillment of the requirements for the Degree of Doctor of Philosophy in Material Engineering.

Signature:

Name: Professor

Dr. Abdul-Wahid Kadhim Rajih

Date:

Signature:

Name: Asst. Professor

Dr.Fadhel Abbas Hashim

Date:

بسم الله الرحمن الرحيم

﴿ وما أوتيتم من العلم إلا قليلا ﴾

صدق الله العظيم

جزء من الآية ٨٥ سورة الإسراء

Abstract

Metals-to-ceramics bonding are increasingly important in so many advanced technological applications such as military, aerospace industries, electronic devise and other important fields.

This study probably represents a real challenge since, many difficulties and set back obstructed are associated metal-to-ceramic bonding processes, due to the sharp difference in characteristics of these materials.

The aim of this study was to join ceramic(٩٩.٨٪Al_2O_3) to copper (٩٩.٨٣%) by active brazing process, the shapes of both materials are cubic(١٤x١٤x١٠)mm, The active filler metal well selected in two alloying systems: Cu-Ti and Cu-Ti-Co and it was prepared as a past form.

Bonding processes were carried out under inert gas (argon). The effects of active element(Ti), temperature and holding time on microstructure, reaction products and bonding strength were studied.

Bonding processes were conducted at temperatures of (٩٥٠, ٩٧٥, ١٠٠٠, ١٠٢٥, ١٠٥٠) ^oC ,Titanium contents were(١٠, ٢٠, ٣٠, ٤٠, ٥٠, ٦٠) % and for periods of time (١٠, ١٥, ٣٠, ٤٥, ٦٠)min.

Results obtained showed that the bonding strength depends mainly on titanium percentage, temperature at which bonding process was carried out and holding time.

The highest bonding strength(٢٨MPa) was obtained in Cu-٤٠wt%Ti system. Fracture occurred partly at the layer in contact with alumina.

However, when ٥wt%Co was added at ١٠٢٥ ^{o}C for ٣٠min,the strength reached a maximum value of ٤٤.٥ MPa, i.e. an improvement of ٥٧٪ occurred. The fracture then, happened totally in the alumina part.

The addition of cobalt however, introduces further changes including: thickness, nature of layer bonding and diffusion zone. This addition creates an arrangement of composition in the bonding region similar to the graded coating which results in minimizing of induced stresses due to the sharp difference in thermal expansion between copper and alumina and eventually results in chemical of bonding stability and mechanical keying.

X-Ray analysis of the copper-alumina joints revealed the formation of TiO (monoclinic),$Cu_{٢}Ti_{٤}O$(cubic)and $Co_{٢}Ti_{٤}O$(cubic) compounds at the interface.

The behavior of graded coating-like-observed may be attributed to these compounds and the diffusion zone region.

High thermal shock resistance was observed in the examined(optimum)samples during water quenching and air cooling from(٤٠٠, ٥٠٠, ٦٠٠, ٧٠٠) ^{o}C .This result indicated high bonding strength, good adhesion and plasticity of the reaction layers.

A theoretical model (FEM) was built and implemented by using ANSYS ٥.٤ software package to predict the magnitude of residual stresses during cooling the braze joints..

الخلاصة

تكتسب عمليات ربط المواد المعدنية بالسيراميك أهمية متزايدة في استخدامات تكنولوجية متقدمة كالصناعات العسكرية وصناعات الفضاء والأجهزة الالكترونية الدقيقة ومجالات شتى عديدة.

هذه الدراسة ربما تمثل تحدياً حقيقياً لصعوبات بالغة تكتنف عمليات الربط بين المعدن والسيراميك نظراً للتباين الحاد في الخواص بشكل عام ولعل هذه الدراسة هي الأولى في العراق لربط المعدن (النحاس ٩٩.٨٣%) بالسيراميك(الومينا ٩٩.٨%) بطريقة اللحام بالمونة الفعالة ظروفاً ومحددات. كلا المادتين على شكل مكعب (١٤ملم x ١٤ملم x ١٠ ملم)وتم اختيار مادة المونة الفعالة بنظامين : (نحاس- تيتانيوم) ، (نحاس- تيتانيوم – كوبلت) وحضرت مادة الحشو على شكل عجينة.

أجريت عمليات الربط في ظروف حماية بالغاز الخامل(الآركون) ، كما تمت دراسة تأثير محتوى العنصر الفعال(التيتانيوم)، درجة الحرارة والزمن على البنية المجهرية ونواتج التفاعل ومقاومة الربط.

تم اختيار درجات حرارة الربط كالتالي : (٩٥٠، ٩٧٥ ، ١٠٠٠، ١٠٢٥، ١٠٥٠) C^{o} وعند نسب مختلفة من التيتانيوم (١٠،٢٠،٣٠،٤٠،٥٠،٦٠) wt% ولفترات زمنية(١٠،١٥،٣٠،٤٥،٦٠)دقيقة. أظهرت النتائج أن مقاومة الربط تعمد بشكل رئيسي على نسبة العنصر الفعال(التيتانيوم)ودرجة الحرارة التي أجريت فيها عملية الربط وزمن المكوث.

في نظام (Cu-٤٠wt%Ti) كانت أعلى قيمة لمقاومة الربط في حدود(٢٨ MPa) إذ حدث الكسر جزئياً في الطبقة الملامسة للألومينا.أما عند أضافة ٥wt% Co للسبيكة Cu-٤٠wt%Ti وعند درجة حرارةC^{o} ١٠٢٥ ولفترة مكوث ٣٠ دقيقة كانت مقاومة الربط هي (٤٤.٥ MPa) ،حيث حدث تحسنا بنسبة ٥٧% , إذ كان الكسر كلياً في منطقة الألو مينا.

إضافة الكوبلت أحدثت تغيرات أخرى شملت السمك أو طبيعة طبقة الربط وكانت أقصى مقاومة للربط عند سمك ٢ µm.التغير في شكل وطبيعة وسمك طبقة الربط والمنطقة الانتشارية (Diffusion Zone)أحدثت مايشبه تدرجاً في الطبقات بخواص مختلفة سببت انخفاضا في التباين لمعاملات التمدد الطولي مما قلل من الأجهادات الحرارية وأستقرارية الربط الكيمائي والميكانيكي Mechanical Keying).

أجريت اختبارات الأشعة السينية لتحديد نواتج التفاعل وهي كالآتي: أوكسيد التيتانيومTiO (أحادي الميل) ومركبات الربط Cu_2Ti_4O(مكعب) ،Co_2Ti_4O(مكعب)،وربما إليها والى منطقة الانتشار يعزى التدرج في معاملات التمدد الطولي وآلية الربط.

أبدت النماذج مقاومة عالية للصدمة الحرارية من درجات حرارة عالية(٤٠٠،٥٠٠،٦٠٠،٧٠٠) ^oC بما يؤشر وجود قابلية ربط قوية وغياباً لتأثير التباين في معاملات التمدد.

تم بناء نموذج نظري بطريقة العناصر المحددة وتم تنفيذه باستخدام نظام التحليل ANSYS ٥.٤ للتنبؤ بالأجهادات المتخلفة خلال تبريد وصلة اللحام .

Appendix A

Diffraction data cards for the following components are:

١- α-Al_2O_3 , Alpha aluminum oxide (Corundum).

٢- Cu , Copper.

٣- Ti , Titanium.

٤- TiO , Titanium oxide.

٥- TiO_2 , Titanium oxide (Anatase).

٦- Cu_2Ti_4O , Copper titanium oxide.

٧- Cu_3Ti , Copper titanium

٨- Co_2Ti_4O , Cobalt titanium oxide

٩- Co_2Ti Cobalt titanium

10-173 MINOR CORRECTION

d	2.09	2.55	1.60	3.48
I/I_1	100	90	80	75

α-Al_2O_3

ALPHA ALUMINUM OXIDE (CORUNDUM)

Rad. $CuK\alpha_1$ λ 1.5405 Filter Ni Dia.
Cut off I/I_1 DIFFRACTOMETER
Ref. NAT. BUR. STANDARDS (U.S.) CIRC. 539 9 3 (1959)

Sys. TRIGONAL S.G. D_{3D}^6 - $R\bar{3}c$ (167)
a_o 4.758 b_o c_o 12.991 A C 2.7303
α β γ Z 6 Dx 3.987
Ref. IBID.

$\xi\alpha$ $n\omega\beta$ $\xi\gamma$ Sign
2V D mp Color
Ref.

SAMPLE ANNEALED AT 1400°C FOR FOUR HOURS IN AN Al_2O_3 CRUCIBLE. SPECT. ANAL. SHOWED <0.1% K,Na,Si; <0.01% Ca, Cu, Fe,Mg,Pb; <0.001% B,Cr,Li,Mn,Ni.
CORUNDUM STRUCTURE.
PATTERN MADE AT 26°C.

d Å	I/I_1	hkl	d Å	I/I_1	hkl
→3.479	75	012	1.1382	2	311
→2.552	90	104	1.1255	6	312
2.379	40	110	1.1246	4	128
2.165	< 1	006	1.0988	8	0.2.10
→2.085	100	113	1.0831	4	0.0.12
1.964	2	202	1.0781	8	134
1.740	45	024	1.0426	14	226
1.601	80	116	1.0175	2	402
1.546	4	211	0.9976	12	1.2.10
1.514	6	122	.9857	< 1	1.1.12
1.510	8	018	.9819	4	404
1.404	30	124	.9431	< 1	321
1.374	50	030	.9413	< 1	1.2.11
1.337	2	125	.9345	4	318
1.276	4	208	.9178	4	229
1.239	16	1.0.10	.9076	14	324
1.2343	8	119	.9052	4	0.1.14
1.1898	8	220	.8991	8	410
1.1600	< 1	306	.8884	< 1	235
1.1470	6	223	PLUS 11	LINES	TO .7931

4-0836 MAJOR CORRECTION

d 4-0846	2.09	1.81	1.28	2.088	Cu
I/I_1 4-0836	100	46	20	100	COPPER (COPPER)

Rad. CuKα_1 λ 1.5405 Filter Ni
Dia. Cut off Coll.
I/I_1 G. C. DIFFRACTOMETER d corr. abs.?
Ref. SWANSON AND TATGE, JC FEL. REPORTS, NBS (1949)

Sys. CUBIC S.G. O_H^5 - FM3M
a_o 3.6150 b_o c_o A C
α β γ Z 4
Ref. IBID.

ε α n ω β ε γ Sign
2V D_X 8.936 mp Color
Ref. IBID.

JOHNSON AND MATTHEY-SPEC. SAMPLE, ANNEALED AT 700°C IN VACUUM.
AT 26°C
TO REPLACE 1-1241, 1-1242, 2-1225, 3-1005, 3-1015, 3-1018

d Å	I/I_1	hkl	d Å	I/I_1	hkl
2.088	100	111			
1.808	46	200			
1.278	20	220			
1.0900	17	311			
1.0436	5	222			
0.9038	3	400			
.8293	9	331			
.8083	8	420			

5-0682 MINOR CORRECTION

d	2.24	2.56	2.34	2.557	Ti
I/I_1	100	30	20	30	TITANIUM

Rad. $CuK\alpha_1$ λ 1.5405 Filter Ni
Dia. Cut off Coll.
I/I_1 G.C. DIFFRACTOMETER d corr. abs.?
Ref. SWANSON AND FUYAT, NBS CIRCULAR 539, VOL. III, (1953)

Sys. HEXAGONAL S.G. D_{6h}^4 - $P6_3/MMC$
a_o 2.950 b_o c_o 4.686 A C 1.588
α β γ Z 2
Ref. IBID.

ε α n ω β ε γ Sign
2V D_x 4.503 mp Color
Ref.

SAMPLE FROM NEW JERSEY ZINC CO., PREPARED BY THE IODIDE PROCESS. SPECT. ANAL.: .02% AL; .012% FE, MN; .006% MO; .004% N; .0025% MG; .002% CU.
X-RAY PATTERN AT 25°C.

REPLACES 1-1197, 1-1198

d Å	I/I_1	hkl	d Å	I/I_1	hkl
2.557	30	010	0.8005	9	302
2.342	20	002			
2.244	100	011			
1.726	19	012			
1.475	17	110			
1.332	16	103			
1.276	2	200			
1.247	16	112			
1.233	13	201			
1.1708	2	004			
1.1220	2	202			
1.0653	3	014			
0.9895	6	203			
.9458	11	211			
.9179	10	114			
.8927	4	212			
.8796	4	015			
.8634	2	204			
.8514	4	300			
.8211	12	213			

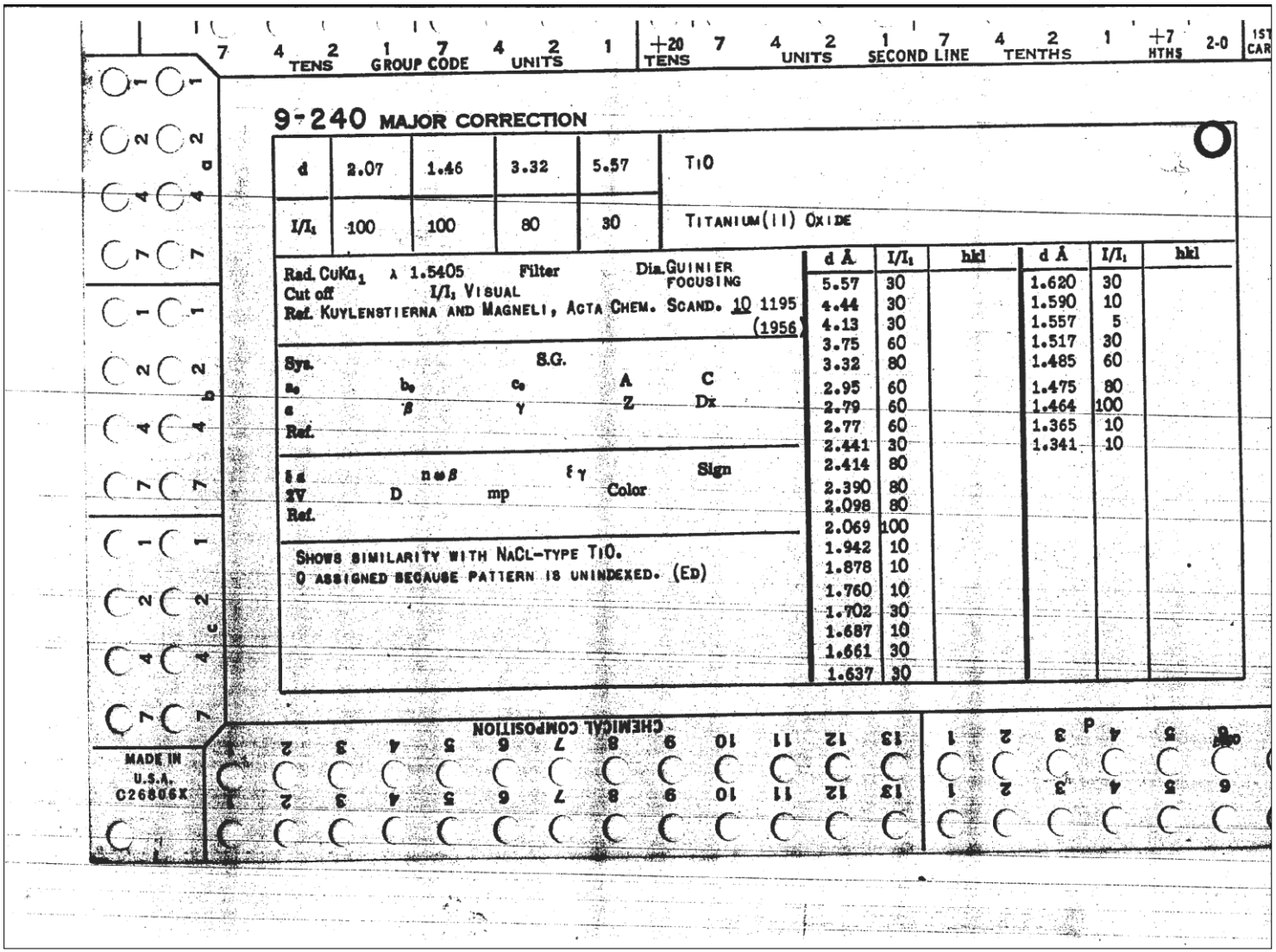

7 4 2 1 TENS 7 4 2 1 GROUP CODE 7 4 2 1 UNITS +20 TENS 7 4 2 1 UNITS 7 4 2 1 SECOND LINE 7 4 2 1 TENTHS +7 HTHS 2-0 1ST CAR

9-240 MAJOR CORRECTION

d	2.07	1.46	3.32	5.57
I/I_1	100	100	80	30

TiO

TITANIUM(II) OXIDE

Rad. $CuK\alpha_1$ λ 1.5405 Filter Dia. GUINIER FOCUSING
Cut off I/I_1 VISUAL
Ref. KUYLENSTIERNA AND MAGNELI, ACTA CHEM. SCAND. 10 1195 (1956)

Sys. S.G.
a_o b_o c_o A C
α β γ Z Dx
Ref.

ε α n ω β ε γ Sign
2V D mp Color
Ref.

SHOWS SIMILARITY WITH NaCl-TYPE TiO.
O ASSIGNED BECAUSE PATTERN IS UNINDEXED. (ED)

d Å	I/I_1	hkl	d Å	I/I_1	hkl
5.57	30		1.620	30	
4.44	30		1.590	10	
4.13	30		1.557	5	
3.75	60		1.517	30	
3.32	80		1.485	60	
2.95	60		1.475	80	
2.79	60		1.464	100	
2.77	60		1.365	10	
2.441	30		1.341	10	
2.414	80				
2.390	80				
2.098	80				
2.069	100				
1.942	10				
1.878	10				
1.760	10				
1.702	30				
1.687	10				
1.661	30				
1.637	30				

CHEMICAL COMPOSITION

MADE IN U.S.A. C26806X

N

2.848	Cu_2Ti_4O
1	COPPER TITANIUM OXIDE

er Ni
l. 1/8" x .018"
r. abs.? No
HICAGO, ILL.

- FD3M
C

Sign

CLUDES

HE LAST OF
R THIS

d Å	I/I1	hkl	d Å	I/I1	hkl
2.848	1	400	1.395	5	733
2.602	1	331	1.347	80	660,822
2.326	60	422	1.320	40	555,751
2.258	40	10,431	1.255	20	911,753
2.194	100	333,511	1.245	40	842
2.145	5	520,432	1.233	20	921,761
2.073	20	521			655
2.017	60	440	1.149	80	933,771
1.985	5	522,441			754
1.929	5	531	1.136	5	10,11,
1.902	40	600,442			942
1.789	5	621,540	1.100	40	10.20,
		443			862
1.738	5	533	1.043	5	10.42
1.718	20	622	1.031	20	11.11,
1.648	20	444			775
1.598	40	711,551	0.9952	20	10.44,
1.527	20	642			882
1.485	20	731,553	.9818	5	10.60,
1.429	5	800			866

2059

3.52	TiO_2
100	Titanium Oxide (Anatase)

Dia.

Mono. 25, Sec. 7

$4_1/amd$ (141)
A C
Z 4 Dx 3.893

Color Colorless Sign

d A	I/I1	hkl	d A	I/I1	hkl
3.52	100	101	1.0436	4	321
2.431	10	103	1.0182	2	109
2.378	20	004	1.0070	2	208
2.332	10	112	0.9967	2	323
1.892	35	200	.9555	4	316
1.6999	20	105	.9464	4	400
1.6665	20	211	.9246	<2	307
1.4930	4	213	.9192	2	325
1.4808	14	204	.9138	2	411
1.3641	6	116	.8966	4	219,1110
1.3378	6	220	.8890	2	228
1.2795	<2	107	.8819	<2	413
1.2649	10	215	.8793	2	404
1.2509	4	301	.8464	2	420
1.1894	<2	008	.8308	<2	327
1.1725	2	303	.8268	4	415
1.1664	6	224	.8102	2	309
1.1608	4	312	.7974	4	424
1.0600	2	217	.7928	2	0012
1.0517	4	305			

1338

25-316

25-315

d	2.05	2.16	1.97	3.41	$(Cu_3Ti)8\underline{O}$
I/I_1	100	50	40	<2	Copper Titanium

i

Rad. CuKα λ 1.5418 Filter Dia.
Cut off I/I_1 Diffractometer $I/I_{cor.}$
Ref. Giessen and Szymanski, J. Appl. Cryst., 4 257 (1971)

Sys. Orthorhombic S.G. Pmnm (59)
a_0 5.45 b_0 4.42 c_0 4.30 A C
α β γ Z 2 Dx
Ref. Ibid.

εα nωβ εγ Sign
2V D mp Color
Ref.

Metastable phase decomposes at 500°C into $TiCu_4$ and unidentified phase (Ti_2Cu_3?).

d A	I/I_1	hkl	d A	I/I_1	hkl
3.41	<2	110			
3.35	<2	101			
2.325	10	210			
2.207	10	020			
2.163	50	002			
2.046	100	211			
1.971	40	021			
1.580	10	212			
1.545	20	022			
1.361	15	400			
1.296	10	230			
1.222	15	213			
1.207	10	023			
1.153	5	420,402			
1.120	5	421			
1.112	10	232			
1.075	5	004,041			

FORM M-2
W

5-0697 MINOR CORRECTION

d	2.17	1.33	1.13	2.297	Co_2Ti_4O
I/I_1	100	80	80	60	COBALT TITANIUM OXIDE

Rad. Cu λ 1.542 Filter Ni
Dia. 14CM Cut off Coll. 1/8" x .018"
I/I_1 VISUAL INSPECTION d corr. abs.? No
Ref. ROSTOKER, ARMOUR RES. FOUND., CHICAGO, ILLINOIS

Sys. CUBIC S.G. O_h^7 - FD3M
a_o 11.317 b_o c_o A C
α β γ Z
Ref. IBID.

ε α nωβ ℓγ Sign
2V D mp Color
Ref.

d Å	I/I_1	hkl	d Å
2.297	60	422	1.106
2.259	5	500,430	1.092
2.165	100	333,511	1.086
1.989	60	440	1.017
1.902	5	531	0.9822
1.876	40	442,600	.9679
1.696	20	622	
1.626	20	444	.9537
1.574	20	551,711	
1.507	5	642	.9414
1.466	20	650,643	.9316
1.329	80	660,822	
1.303	40	555,751	.9162
1.292	5	662	
1.259	5	840	.8639
1.230	5	911,753	
1.229	40	842	
1.183	5	931	
1.133	80	933,771 (755	

CoTi٢ Cobalt titanium

The main three peaks are ٢.٠٢$_x$ ٢.١٧٥ ١.٩٨٥ File No. ٥-٧١٩

Appendix B

High Temperature Properties of Copper Base Metals used in Finite element models

Young's Modulus

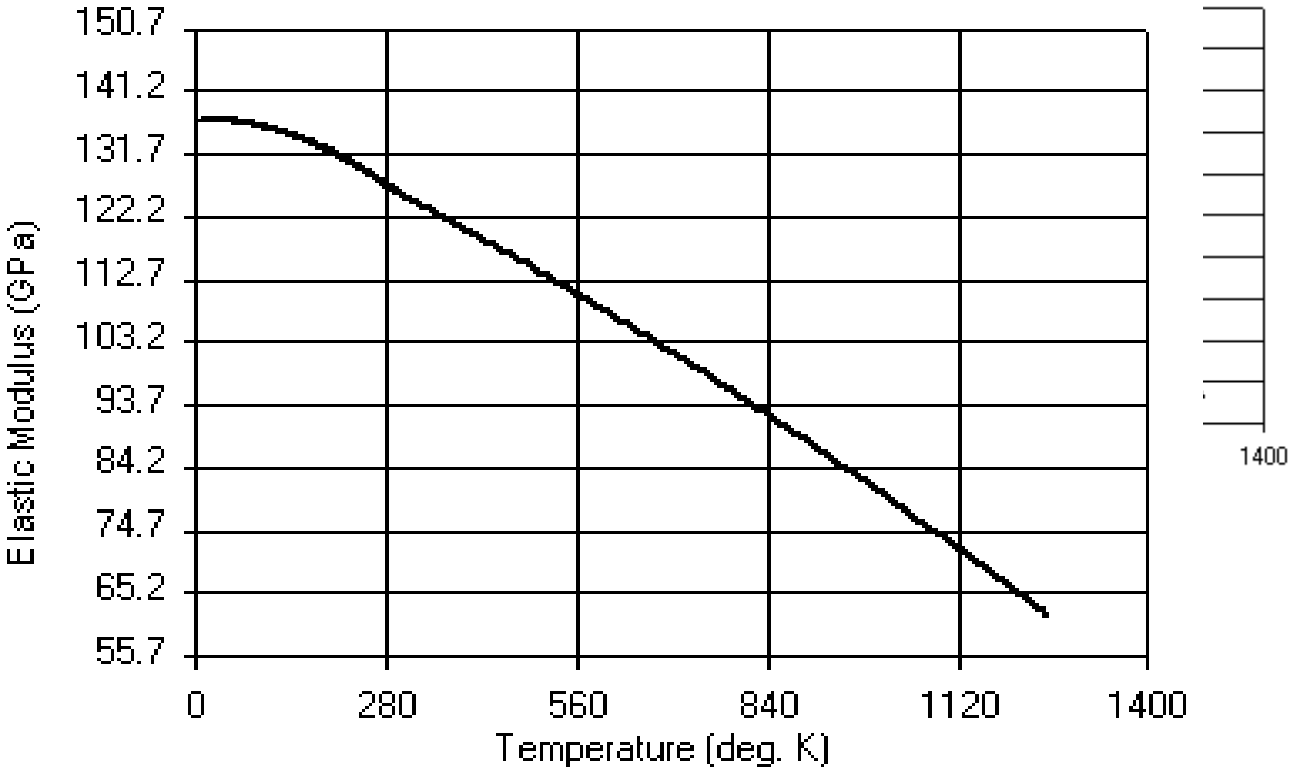
150.7
141.2
131.7
122.2
112.7
103.2
93.7
84.2
74.7
65.2
55.7
Elastic Modulus (GPa)
0
280
560
840
1120
1400
Temperature (deg. K)
1400

Thermal Conductivity

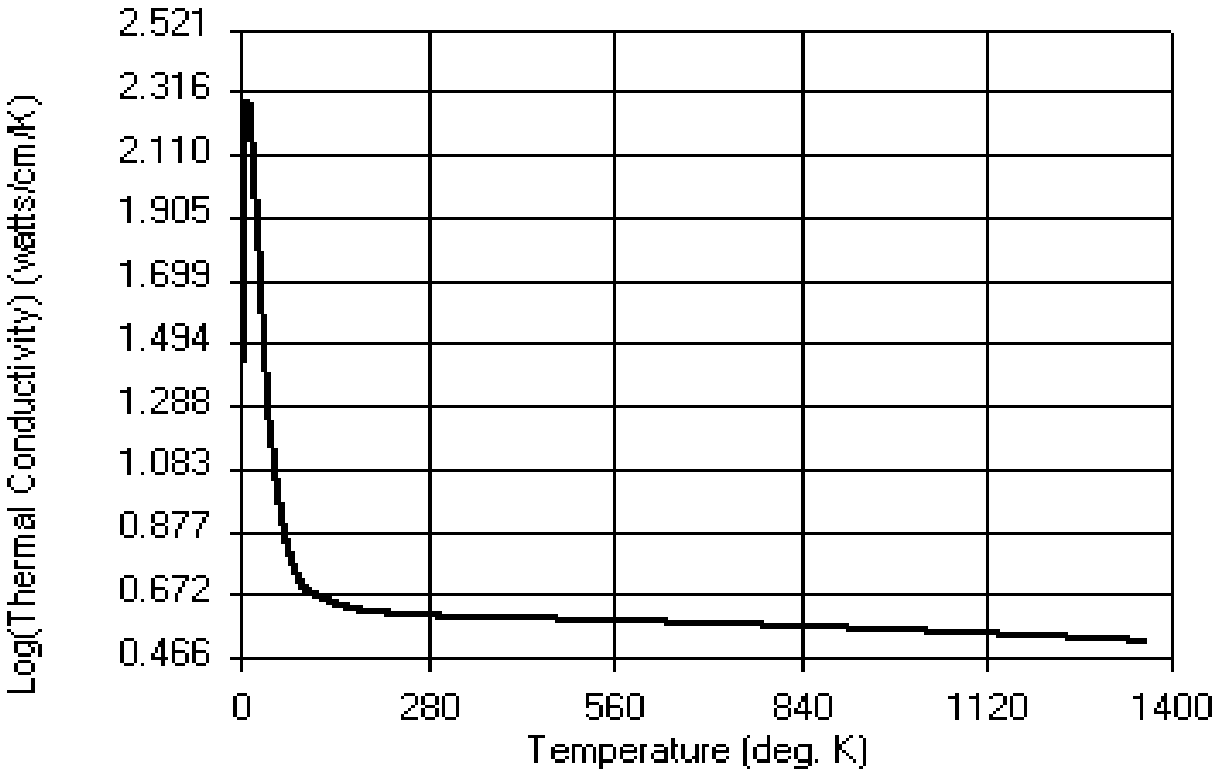

Total Coefficient of Thermal Expansion

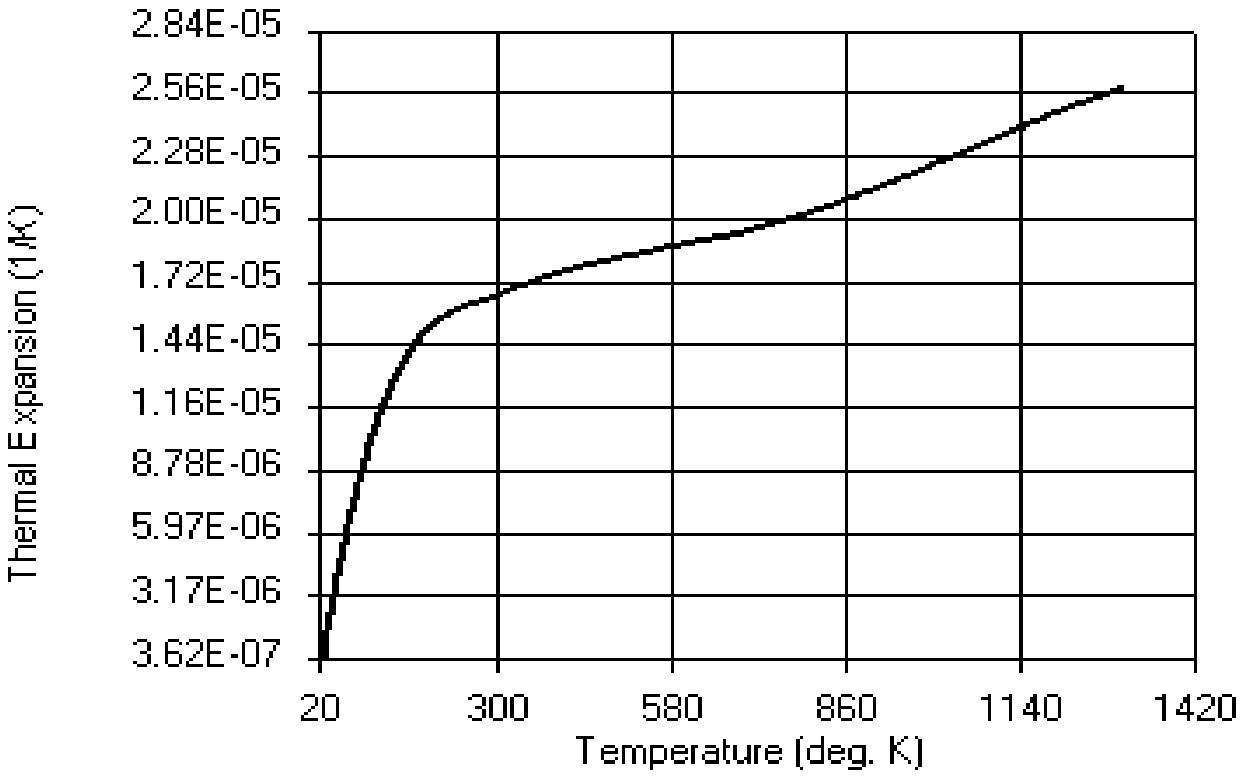

List of Figures

Symbol and Abbreviations

ABA	Active brazing alloy
AISI	America Society for Testing Materials
AWS	American Welding Society
A	Area
A	Defect size; Chemical activity
B	Bulk density, $g/cm^{٣}$
BAg	Silver-base brazing filler metals
BAu	Gold-base brazing filler metals
BCu	Copper- base brazing filler metals
c	Number of components
CTE	Coefficient of thermal expansion ,ppm /^{o}C
D	Dray weight , g
^{٢}D	Two dimensions
^{٣}D	Three dimensions
DBS	Double-brazed shear
D	Average length of diagonal ,mm

E	Internal energy;Young′s modulus
E_c	Young′ s modulus of ceramic component
E_m	Young′ s modulus of metal component
EDS	Energy dispersive spectroscopy
EPMA	Electron prop micro- analyzer
F	Helmoltz free energy
FEM	Finite element method
G	Gibbs free energy
h	Thickness of the metal interlayer
K_I	Intensity factor for mode I, MPa $m^{1/2}$
K_{II}	Intensity factor for mode II, MPa $m^{1/2}$
K_{Ic}	Fracture toughness, MPa $m^{1/2}$
k	Thermal conductivity, W/m.K,material constant
M	Saturated weight , gm
MISES	Von Mises stress .(Pa).
N_i	The amount of component i
OM	Optical Microscopy
P	Pressure; Applied load
PSZ	Partially stabilized zirconia

Q	Activation energy, J/mol
q	Heat flow, Watt
R	Universal gas constant, R=٨.٣١٤ J/mol K
R_a	Roughness average, µm
S	Suspension weight(gm),Entropy
SEM	Scanning electron microscopy
S_x	Normal stress in x-direction, (MPa)
S_y	Normal stress in y-direction ,(MPa)
S_z	Normal stress in z-direction, (MPa)
S_{xy}	Shear stress in x-y plane ,(MPa)
S_{yz}	Shear stress in y-z plane ,(MPa)
S_{xz}	Shear stress in x-z plane ,(MPa)
S١	١^{st} principle stress ,(MPa)
S٢	٢^{nd} principle stress ,(MPa)
S٣	٣^{rd} principle stress ,(MPa)
T	Temperature
t	Time
SIALON	Si-Al-O-N
U	Strain energy, J
V_e	Exterior volume .$cm^{٣}$

W_{ad}	Work of adhesion ,J/ $m^{۲}$
W_{sep}	Work of separation ,J/ $m^{۲}$
X	Thickness of reaction layer,μm
XRD	X-ray diffraction
α	Linear coefficient of thermal expansion $C^{-۱}$
σ	Thermal residual stress
σ_A	Surface energy of solid / vapor interface.J/$m^{۲}$
σ_B	Surface energy of liquid/ vapor interface.J/$m^{۲}$
$\gamma_{A/B}$	Surface energy of liquid/ solid interface.J/$m^{۲}$
$\sigma.$	Uniaxial yields stress
$\varepsilon.$	Yields strain
$\Delta T/\Delta X$	Temperature gradient
μ_i	Chemical potential of element *i*
Ω	Grand potential
θ	Contact angle, degree
ψ	Phase angle, degree
Γ_i	Fracture energy of interface, J/$m^{۲}$
Γ_F	Fracture energy of ductile member(metal), J/$m^{۲}$
Γ_S	Fracture energy of brittle member(ceramic), J/$m^{۲}$
γ	free energy per unit area

ρ_w Density of water (١ gm/cm^{٣})

Table of Contents

List of Tables

Chapter ١

Introduction and Objective

١.١ Introduction

In the past, metals and metals alloy systems were the traditional raw materials for mass production, engineering, and high technology manufacturing. Although ceramics were the second most widely used structural material group after metals, the manufacturing and processing technologies of ceramics have progressed relatively slowly. However, as novel techniques have been developed, ceramics have emerged as engineering materials that are stronger than steels, almost as hard as diamond, and able to withstand high temperatures. Structural applications of ceramics cover air crafts, automobiles,batteries,integrated circuits, cutting tools, and biomaterials.[١-٤].

Although ceramics may posses a unique and desirable set of properties, there will be applications in which these properties are needed and desirable not for entire structure, but only for one portion of the structure. In addition,

the inherently brittle nature of ceramics limit their machanabilty.Therefore, in most structural applications, ceramics are integrated as a critical components in a system that is largely metallic. Hence, ceramics have to be joined frequently to other ceramic parts of metals.Fig.١-١ shows ceramic components integrated in an automotive gas turbine engine and electronic devices[٥]. As shown in Fig.١-١, joining can facilitate the use of structural by limiting them to the most critical portion of the structure. Therefore, reliable joining technologies are essential not only for full exploitation of the properties of the ceramic but also for success of the overall structure.

Achieving high integrity joints between ceramic and metal, however, is a challenge. A major challenge in the commercial utilization of ceramics is reliably joining them to other components in the engineering system. Common technologies used to join metallic components, such as mechanical fastening, welding, or brazing, are not easily adapted to ceramic materials. Brazing, defined by the AWS as "a group of welding processes which produces a coalescence of materials by heating them to a suitable temperature and by using a filler metal having a liquidus above ٤٥٠°C and below the solidus of the base metals." has been identified as one of the most promising techniques for joining ceramics to themselves and metallic components on production scale[٦-٧] .

The challenge of brazing metals to ceramics has both chemical and mechanical components. Ceramic surfaces, especially oxides, carbides and nitrides. are very stable chemically.Cosequently, molten metals do not wet them well because the energy of the molten metal-ceramic interface is grater than the surface energy of the bare ceramic surface, most molten metal bead

up on ceramic surfaces as a water does on wax. One way to overcome the chemical challenge is to use active brazing alloy, i.e. one containing a very reactive metal, such as Ti or Zr ,have been added. It is believed that the reactive element causes the formation semi-metallic oxides and other intermetallic compounds by decomposing a thin surface layer of the ceramic at the ceramic-filler metal interface, which can then be wet by the molten filler metal [٤,٧-٨]

The mechanical challenge of brazing metals to ceramics is overcoming residual stresses caused by the physical property mismatch between the materials. Residual stresses develop when two ceramic component is brazed to a metal component using a filler metal or when a ceramic component is brazed to a metal component using a filler metal. The most pronounced mismatch is in the coefficient of thermal expansion(CTE):most ceramic have CTE_S (٣-١٠) x١٠$^{-٦}$ ⁄ ^{o}C where as typical engineering alloy have CTE_S (١٢-١٨)x١٠$^{-٦}$ ⁄ ^{o}C. Since brazing processes are executed at high temperatures,CTE mismatch causes the components of the joint to contact at different rates during cooling while being fixed at the interface, resulting in residual strains. The ductile filler metal or base metals with low yield stress deforms to accommodate the dimensional mismatch at the interface, however residual stresses in the substrates remain high and the mechanical integrity of the joint is compromised.. The stress state of a brazed joint is difficult to characterize analytically. So finite element methods are frequently employed to calculate the theoretical residual stresses in the ceramic ⁄ metal joint. The simulated stress fields are often used to predict where cracks will initiate and grow[٩-١٠].

A popular ceramic ⁄ metal brazing alloy system is the titanium-copper binary. The titanium reacts very aggressively with oxygen, nitrogen, and carbon

in the ceramic as well as being a nearly universal solvent for metals. The copper is a relatively inexpensive with good flowability and a strong depression of the melting point of titanium. Unfortunately, these alloys contain a relatively large amount of titanium with a high chemical activity. In long term high temperature exposure, the titanium may oxidize at the edge of the joint which is exposed to the atmosphere. Often , it also continues to react with the base ceramic causing decomposition of the bonding interface. Most research to date , has focused on using copper or silver as a base metal of brazing alloy.

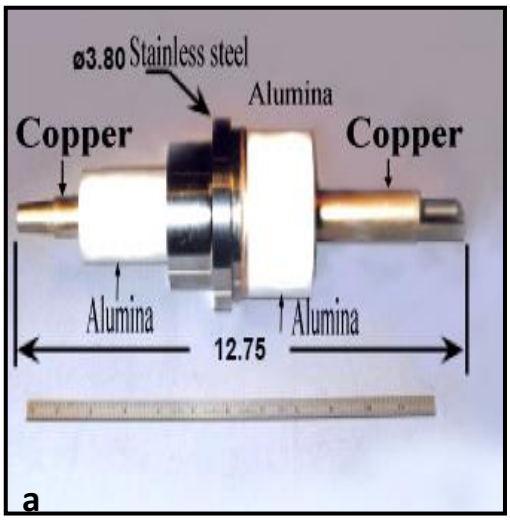

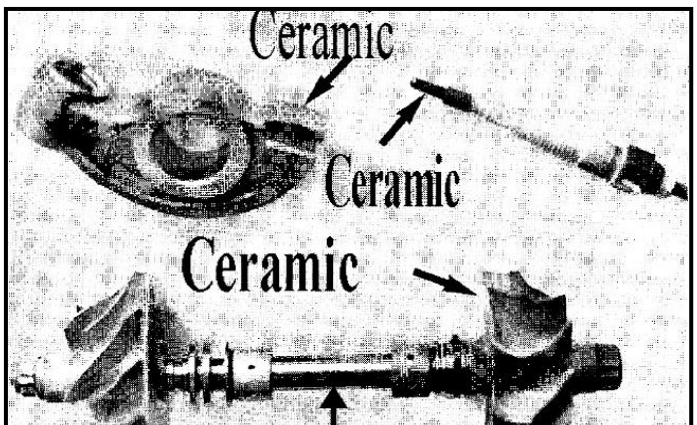

Figure ١-١: Critical ceramic parts in (a,b) electronic device (c)automobile engine components, the turbocharger roter,the rocker arm and the sparking plug[٢,٥,١١-١٢]

The work presented in this thesis focuses on develop the suitable an active metal brazing alloy Cu-Ti and Cu-Ti-Co to join the copper with alumina.

The organization of this work is as follows:

In Chapter ٢, establishes an overview of ceramic-metal joining techniques and suitable brazing alloy developed for ceramic-to-metal. Joining within the last few decades. In Chapter ٣, presents a mechanism of bond formation at the interface , theoretical studies of the effect of residual stresses and factors affecting the strength and fracture of ceramic-to-metal joints. In Chapter ٤, present the experimental procedures and a finite element model as a tool for predicting joint strength**.** In Chapter ٥, the results of experimental and numerical modeling are presented. The conclusions are presented in Chapter ٦.

١.٢ Objective

- Studying the optimal time, temperatures and percent active metal additives, which produce a thin and continuous reaction layer for copper-alumina system.
- Understanding the interface chemical reactions between stable ceramics and reactive liquid metals, and developing microstructures.

- Studying how the reaction layers products affect on the shear strength of copper –to-alumina brazed joints.
- Detecting the phases that play a main role to obtain reliable joint of copper-to-alumina system.
- Studying the effect of additional cobalt element in Cu-Ti based filler metal on alumina-copper system.

braze alloy

- Predicting the maximum residual stresses location in alumina-copper system.

There are many recent advances leading to the usage of copper – alumina composite. The major applications for Al_2O_3/Cu systems include: electronic devices such as IC packages, chip carriers, power transistor modules, high frequency devices and mobile communications.

Chapter ٢

Ceramic – Metal Joining

Processes and Joining Evaluation

٢.١ Introduction

Joining facilitates the use of structure ceramic – as well as other types of ceramic materials- by providing a means to manufacture structure which cannot be made in one piece or which can be made less expensively by joining. Because of their intrinsic brittleness, most ceramics are fabricated by using diverse techniques, thus, avoiding large mechanical loads involved in bulk processing.

Furthermore, ceramic-metal joining is particularly useful when trying to combine the mechanical and/or chemical properties of both ceramics and metals in the same device i.e. ceramic-metal composites, protective coating, etc. Of all the current ceramic-metal joining applications, one of the most important is the attachment of ceramic components operating at high temperatures to structures or moving parts which must withstand stresses or temperature gradients too great for ceramics, and which are usually made of metals.[١٣-١٤].

٢.٢ Joining Techniques

There are a number of techniques for joining materials , of which, bonding temperature is an effective distinguishing feature-Table ٢.١ [٤-٥]. Adhesive, cementicious, and mechanical joining are room temperature techniques, while joining occurs at an elevated temperatures for the other methods. The entire assembly may be heated in the case of brazing, eutectic, and diffusion bonding , or the heating may be localized, as in the case of fusion, induction and friction welding.

Table ٢.١: Comparison of several joining method[٥]

Low temperature processes

Property	Adhesive	Cement	Mechanical
Strength (MPa)	٢٠-٨٠	<١٠	١٠-٥٠
Maximum Temperature (°C)	١٧٥		٥٢٥
Cost	Low	Low	Low-medium

High temperature processes

Property	Brazing	Eutectic	Diffusion	Fusion	Friction
Strength (MPa)	١٠٠-٥٠٠	٢٠٠-٤٠٠	١٠٠-١٠٠٠	٥٠-٢٠٠	٥٠-٢٠٠
Maximum Temperature (°C)	٥٢٥	٩٢٥	١٠٢٥	١٠٢٥	٢٢٥
Cost	Low-medium	Medium	Medium-high	Low-high	Low-medium

As a way of summarizing the broad spectrum of possible ceramic-metal joining techniques, one can classify them into one of the allow major groups: Fig.٢-١ [٤-٥,١٥]

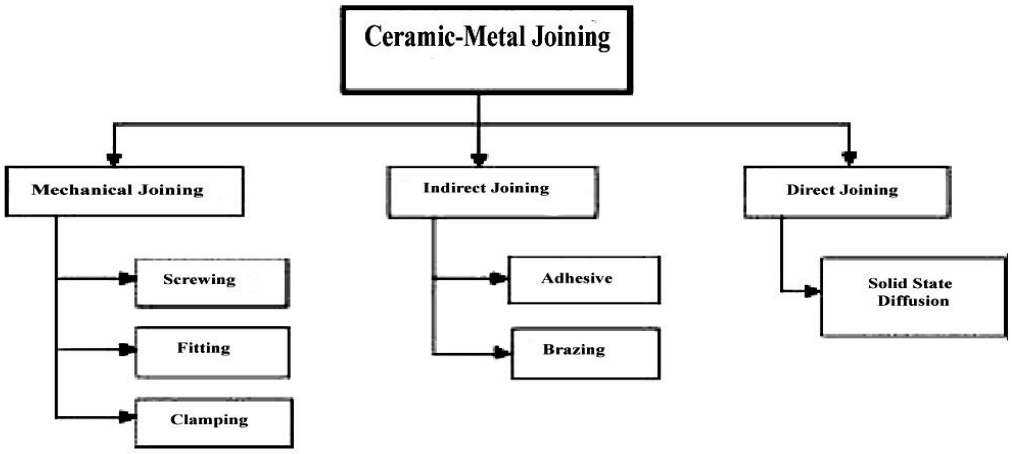

Figure ٢-١: Ceramic-metal joining processes [٥].

٢.٢.١ Mechanical Joining

Mechanical joining are used in both traditional and new application such as securing of furnace roof refectories with metal hooks, fastening, clamping and press-and-shrink fitting is another type of mechanical technique that is widely employed in mass production processes. Typical mechanical strength of the joints vary from ١٠-٥٠ MPa. Stress concentration area (especially in the ceramic counterpart) and design limitation are among the major restrictions of the methods [٥,١٥]

٢.٢.٢ Direct Joining

This technique achieved by pressing together very flat surfaces to achieve bonding. In this type of processes, no intermediate materials(such as a filler alloy) are needed to create a joint between dissimilar materials[٥,١٥].

٢.٢.٢.١ Diffusion Bonding

Solid-state diffusion is a well-known example of direct ceramic-to-metal joining process. In diffusion bonding, base materials with carefully prepared surfaces are held in close contact as high pressure is applied and bonding occurs at temperature below the melting point of the base metal. The process is often performed in a vacuum or a protective atmosphere.Sucessful bonding relies on the achievement of adequate contact, subsequent diffusion, and plastic flow of the metal to eliminate un-bonded areas or interfacial porosity[٢]. Close tolerances and high mechanical strength (١٠٠-١٠٠٠ MPa) are usually attained. In addition to that, admissible working temperatures are imposed by the base materials instead of the interface. Temperatures in excess of ١٠٠٠°C are often possible for SiC-$Si_٣N$-and $Al_٢O_٣$- metal joints[١٨].Inserts of ductile metal foils are often used to accelerate the bonding process by enhancing deformation and reducing the joining temperature Hot –pressing or hot-isostatic pressing are normally used to produce planar joint [٥,٧,١٣,١٥].

٢.٢.٢.٢ Friction Welding

Friction welding is another example of solid state joining Fig.٢-٢ [٥,١٧]. Application in ceramic-metal joining is still in its early stages of development. Successful $Al_٢O_٣$/aluminum alloys joints have been reported [١٨]. Firstly, one of joining surfaces is rotated, the joining surfaces are slightly pressured together and frictioned against each other, resulting in enough heating and joining of the couple. The relative movement is the interrupted and the normal force is increased. This process can be carried out using conventional friction welding apparatus but under a protective atmosphere to avoid metal oxidation. The components to be joined (especially the ceramic) must be planar and parallel to avoid crack formation and propagation as well as joining imperfections. These defects can be originated from uneven heating of non-parallel surfaces.

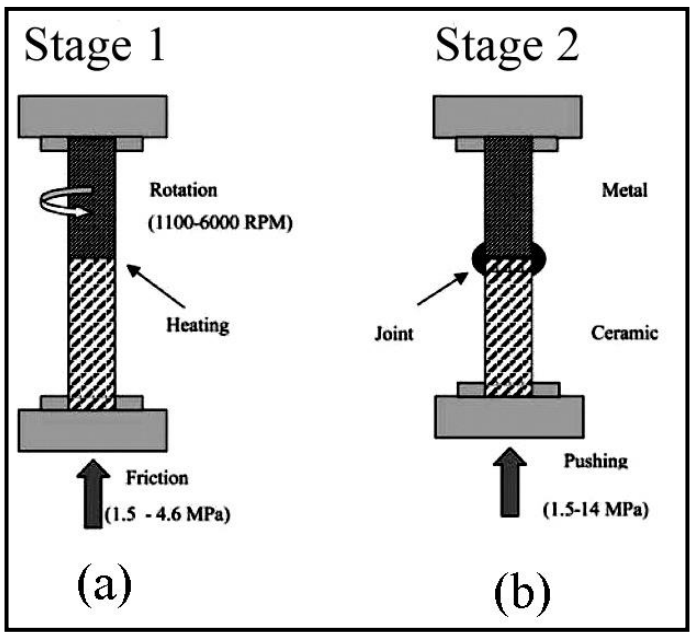

Figure ٢-٢: Schematics of friction welding [١٧]

٢.٢.٢.٣ Fusion Welding

Fusion Welding is a direct joining method based on the localized melting of the metallic component. Techniques that employ localized heating, such as electron – beam or arc-welding are often not suitable for joining dissimilar materials. The high heat generated creates a localized molten region which fuses the surrounding materials together on colddown. This requires an acceptable fracture toughness and thermal shock resistance which brittle material, such as ceramics and intermetallics do not generally posses. A laser beam is commonly used as heating source. The resulting joints normally reach a mechanical strength between ٥٠ and ٢٠٠ MPa at the temperature in excess of ١٠٠٠°C (depending on the base materials). On the downside, grain growth and residual stress development may also occur [٥,١١]

٢.٢.٣ Indirect Joining

Joining processes which require the use of filler materials, such as adhesive joining and brazing ,are commonly referred to as indirect joining processes[٥]. In these types of processes, an intermediate material (such as filler alloy) is used to promote a physical or a chemical bonding between counterparts. There are two main types of indirect joining to joint ceramic – to- metal:

٢.٢.٣.١ Adhesive Joining

The adhesion used for joining ceramic to metal, are either cold cured or hot cured. Adhesive joining using organic interlayers offers suitable mechanical strength below ٢٥٠°C Table ٢.٢. Glassy interlayers can also be used to improve high temperature resistance. Examples of adhesive joining

include magnetic ceramics in electric motors as well as ceramic lining to oil ducts. In the latter case, ceramics are used as protective barrier against corrosion or wear. Glassy interlayers have been long to join Al_2O_3 to Nb in sodium vapor light bulbs (٥,١٥.١٨] .

Table ٢.٢: Organic adhesives used in ceramic / metal joining[٥].

Adhesive	Setting	Maximum Working Temperature (°C)
Epoxy	Hot	١٧٠-٢٢٠
Polyurethane	Hot + cold	١٢٠-١٨٠
Silicon	Cold	١٨٠-٢٢٠
Cyanocrilate	Cold	١٥٠-٢٥٠
Elastomer	Hot	٩٠-١١٠

٢.٢.٣.٢ Brazing

In the case of brazing ceramic-ceramic and ceramic- metal joints may be obtained in two different ways: (i) indirect brazing where the ceramic surfaces are metallized prior to brazing. (ii) direct brazing where the filler alloys contain active elements such as titanium.

A- Metallizing

Ceramic surfaces are relatively not wetted by conventional liquid alloys. To solve this problem, several methods have been developed one of which is metallization of the ceramic surface prior to conventional brazing, since metallized ceramics can be brazed to metals without active alloys. In metallizing a thin layer of metalizing material with few microns link is bonded to the mating face of the ceramic work-piece. The metallized ceramic pieces can then be joined together or to a metal part by brazing, soldering , or in some cases adhesive bonding.

The choice of suitable metallization technique should take into account the base materials involved and microstructual characteristic of the ceramic as well as availability of equipment and intended purpose of the joint [١٩-٢١]

Several techniques of metallizing are available , such as thermal spraying , electrolytic coating, electron-beam and laser coating, vapor phase deposition (chemical or physical) and hot isostatic pressing. The techniques most commonly used are, however, the moly-manganese [١٩.٢٢-٢٣]

Finally, the mechanical metallization is new, simple, and fast method to metallize ceramic. It is developed and patented by the Julich Research center, in German. The process has been initially studied for the metallization of alumina and Zirconia with Ti [٤,٢٤-٢٥]

Joining of metallized ceramic can subsequently be performed with convential brazing alloy (typically BCu, BAg and BAu alloys according to the American welding society specification AWS A٥.٨.٨٩ ١٩٨٩)[٢٦].

The brazing through pre-metallization is a multi-step process and is quite cumbersome. The strength of the joint is very sensitive to the quality of surface pre-treatment and to the effectiveness of the fluxing agents used in the process[٢٦].

B- Active Filler Alloys

In brazing of ceramics, an important alternative to brazing through pre-metallization is active metal brazing. The technique developed at General Electric. Active metal brazing uses special braze alloys that contain an “active metal” particular Ti and sometimes Hf or Zr. Fig. ٢-٣ shows the metallizing method which is called a multi stage method in comparison with actively brazing method which is called a single stage method.

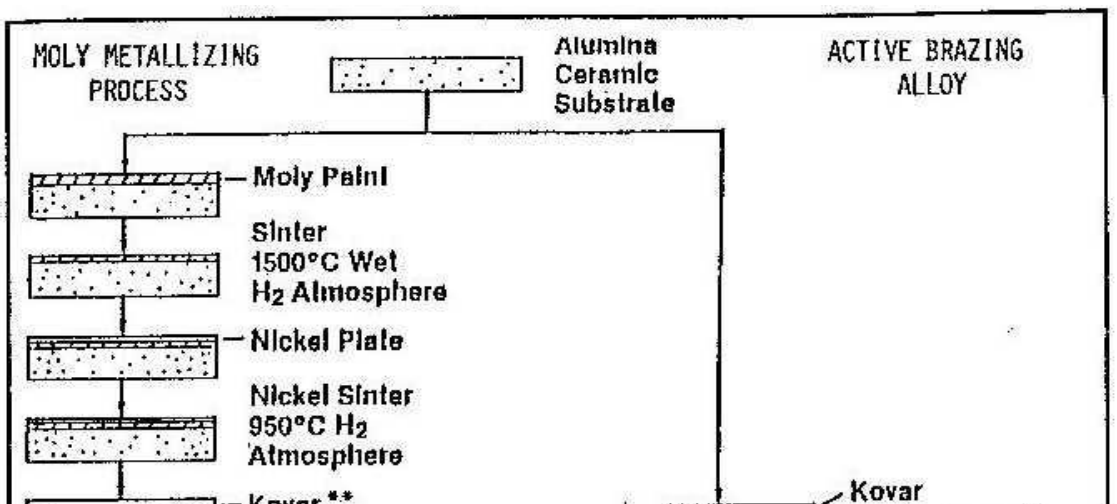

Figure ٢-٣: Comparison of active metal brazing with Mo-Mn process[١٤].

The role of the active metal such as titanium is to react with the ceramic, creating a layer of a reaction product that is more wettable by the metal braze than the original ceramic surface. No pre- metallization is necessary, and the joint can be made in one step.

Active filler alloys for direct ceramic- metal brazing should depict some essential features in order to improve interfacial microstructure, such as: [١٦,٢٧-٢٨]

١. Melting point or melting range compatible with those of base materials;
٢. Moderated fluidity at the brazing temperature, promoting capillarity and uniform distribution over the joint but preventing infiltration into sintered base materials (both metals and ceramics).
٣. Homogeneous composition and stability to minimize constituent separation or segregation upon melting and solidification (brazing cycle);
٤. Thermodynamic compatibility with the base metal surfaces promoting wetting;
٥. Limited trend to brittle phase formation (usually intermetallics)
٦. compatibility with the working temperature, mechanical loading, environment, and intended life span for the joint.

C- Filler Metal Alloy Forms

Active braze alloys are available commercially in several differing forms. To apply the filler metal between the ceramic surfaces, there are four recognized active element joining processes;

١. **Mixed Powders**: Titanium or titanium hydride powder can be mixed with conventional braze alloy powders to form a slurry with a binder. Titanium hydride decomposes at around ٥٠٠^{o}C into metallic titanium to form the active element. The mixture is applied to the surface of alumina and dried. A metal or ceramic member is placed over the coated area and the assembly is heated to brazing temperature in either vacuum or inert gas [٢٩-٣١].

٢. **Coated Ceramics**: A simple method is to deposit a titanium layer onto the ceramic, and braze using a conventional braze alloy system. Deposition methods can be sputter coating ,thin foils titanium brush or screen paints. and then the assembly is heated to the flow temperature. [٣٢].

٣. **Clad Filler Metals** The third commercially available material is a cladded product, which consists of an active element such as titanium cored wires or a titanium "sandwich" foil are also made commercially. These products have the additional advantage over the previous two types because the titanium is protected from the outgassing products during furnace heating by the conventional braze alloy cladding. The disadvantage is that the active metal is not exposed to the ceramic surface until melting has taken place, which gives a poor initial wetting contact angle, and can sometimes lead to a complete failure in the technique

٤. **True ABA alloys**: Modern manufacturing techniques have enabled a whole series of true alloy to be produced with a wide range of melting temperatures .These alloys are partially protected by the other alloy constituents, but do require a very clean (low $PO_٢$) furnace atmosphere. The fourth product is having a controlled quantity of titanium available for joining to the ceramic at the onset of meeting. The loss of the active element is limited to the element found on the outer layer of the brazing metal [١٩].

In this research the first case was used in this investigation because other methods is not easy manufacturing and need a progressive equipment like electron beam melting and casting machine for homogeneity of final product .

D- Development of Active Filler Metals

In the last two decades, the major impetus in brazing of ceramics has been the development of filler metals with improved wettability, eliminating the need for premetallization. These mainly consist of two groups of alloys, i.e. **Cu-X** [٣٣-٣٧] Or **Ag-Cu-X** brazes [٣٨-٤٠],where X is typically a group IVB element (Ti, Zr, Hf), and Ti-Zr alloys[٤١-٤٣] , in many cases, active brazing also contain additions of Ni, Be, Cr, V, In and Co [٧,٤٤-٤٧].

(i) Silver – Copper Filler Metal Alloys

In Ag- based alloys, the solubility of a metal such as Ti is relatively low at relevant brazing temperatures (٩٥٠-١٠٥٠)°C. In contrast, the solubility of Ti in Cu is much higher, which makes the

combination of Ag and Cu attractive for many ceramics contain active elements which promote wetting by decomposing a thin layer at the ceramic surface. The improved wetting of silicon nitride, silicon carbide and alumina as a result of titanium additions to fillers is shown in Fig. (٢.٤). Apparently , about ١٠ at%Ti is sufficient to wet silicon nitride (١١٠٠°C) and silicon carbide (١٠٠٠°C), while ٣٠ at % is required to obtain a similarly low contact angle on alumina (١١٠٠°C). It is reasonable to suggest that this observation is closely linked to the higher thermodynamical stability of aluminum oxide. As a consequence of the low solubility of Ti in Ag, the use of Ag-Cu based alloys should be recommended when brazing alumina[٧].

The Ag-Cu-Ti alloys are based on titanium additions to the eutectic composition of Ag-Cu (٧٨ at % Ag-٢٢ at %Cu), which provides sufficient fluidity of the alloy, since the melting range is relatively narrow. The addition of Ti to Ag-Cu alloys results in minor changes of the melting temperature only (T_M between ٧٥٠ and ٨٥٠°C), which is essential to avoid high temperature brazing[٧].

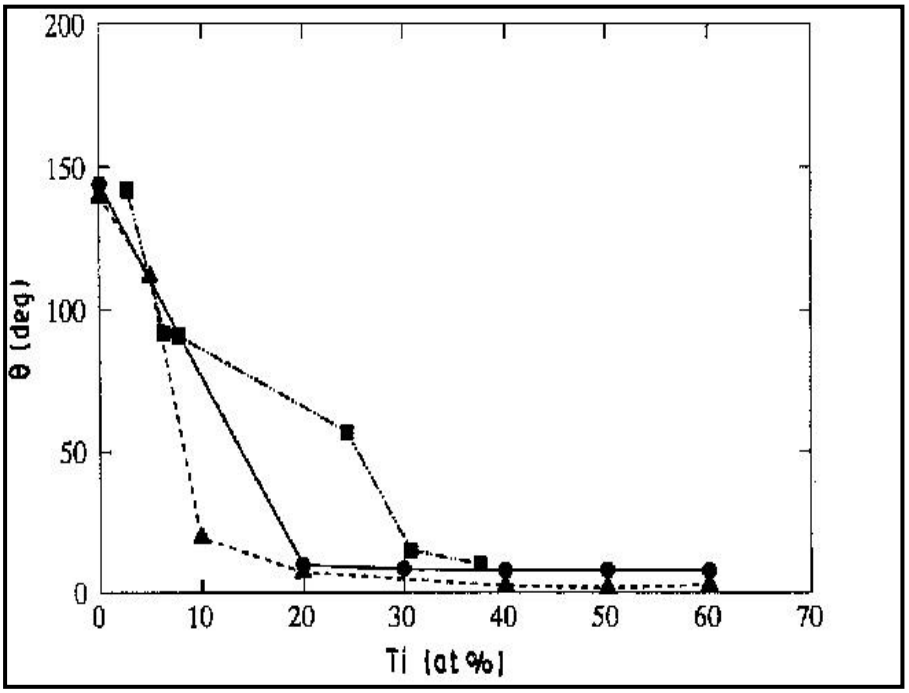

Figure ٢-٤: Effect of filler-titanium content on contact angle θ for (●) Si_3N_4 (١١٠٠°C),(▲) Sic, (١٠٠٠°C) and (■) Al_2O_3 (١١٠٠°C), (data from[٧], [٤٠] and [٤١] respectively).

Several investigations used Ag-Cu brazes to produce ceramic/ metal joints:

H. Mizuhara *et al*., [٤٨] used an active braze alloy manufactured commercially (GTE's ABA alloy) to produce ceramic/ metal Joints. A brazing matrix study was carried out on several alloys produced using the Ag-Cu eutectic as a base material and adding to it differing amount of titanium. These alloys were produced by melting, casting and then rolling them into foil. Brazing was carried out at ٨٢٠°C for ١٠ minutes under ١.٣٣×١٠^{-٦}KPa vacuum. Peel tests were conducted on two different grades of alumina joints to kovar. The results indicate that ٢٪ Ti in Ag-Cu eutectic ally leads to high peel strength, with a higher titanium content the hardness of the alloy increases and hence it exhibits poor peel strength. The peel test results also emphasize the importance of ceramic surface finish. Grinding the ceramic resulted in surface and subsurface damage. Refining at ١٦٥٠°C prior to brazing reduced the machine induced damage. Hence the refried specimens exhibited a higher strength. Removal of the damaged layer by lapping also lead to higher strength. Similar results were found when Si_3N_4 was joined to copper wherein the peel strength of lapped Si_3N_4-Cu joints was twice that of the ground Si_3N_4-Cu surface.

The tensile tests conducted on these joints resulted in failure within the main body of ceramic, indicating that the joint was stronger than the base material.

Thus the study has shown that direct brazing using Ag-Cu eutectic + ٢٪ alloy as a brazing alloy can yield joints equal in strength to the joints made by the moly-manganese process. The Ag-Cu eutectic + ٢٪ Ti alloy developed in this study is currently one of the most popular commercially available brazing alloys.

Mizuhara and Hubel [١٩] emphasized that the brazing alloy should flow in a controlled fashion on the ceramic and not "blush". In certain cases it has been found that the small amount of brazing alloy in a wetting test flow all over the ceramic , slop over this edges and creep underneath too. They termed this phenomenon as "blushing" it is indicative of high degree of capillary action by the alloy.

Mizuhara, Huebel and Oyama [٤٨]]used a double – brazed shear (DBS) test to evaluate a joint between alumina and alloy ٤٢ [Fe-٤١Ni] by using a cusil ABA(٦٣wt.%Ag-٣٥wt%Cu-٢wt%Ti) as a filler metal alloy. They studied the effect of ceramic finishing and thickness of filler metal on DBS test. They have found that the ground ceramic has a lowest shear strength (٦.٢ MPa), However in the ground ceramic and sintered the DBS become (٢٦.٥ MPa). They also showed that the shear strength increased with increasing the thickness of filler metal up to ١٠٠μm and then fall when the thickness is ١٥٠μm. The explanation for these results, first, the thicker filler metal contains more titanium atoms available to bond with the ceramic. Second, the thicker filler metal provides more plastic deformation during the cooling cycle to result in lower thermal stress at the joint.

(ii) Aluminum- Matrix Filler Metal Alloys

In addition to titanium and zirconium, attempts have been made to develop aluminum-based alloys [٧,٤٩] The results indicate that the contact angle on alumina is relatively high compared with that of titanium-containing alloys. Considering the low surface free energy of liquid pure aluminum at the melting temperature, a relatively low work of adhesion may occur. This observation implies that brazing with aluminum fillers may required a high temperature (minimum ١٠٥٠°C), For practical purposes, a contact angle between ٧٠° and ٩٠° may be insufficient to provide satisfactory spreading, and hence a low bond strength level may appear. As a consequence, the use of such fillers may be critical. On the other hand, wetting of alumina can be enhanced by additions of copper to the aluminum filler. In this situation, the contact angle approaches ٥٠° for copper amounts between ٤ and ٣٠ wt% [٧]

Within this range of Cu content the solidification range is between ٠ and ٢٠٠°C, and no intermetallic phases are formed (these are connected with the Cu-rich side of the Al-Cu binary system)[٧]. A similar contact angle has been observed in the wetting of zrconia at ١١٠٠°C (>١٠٠٠s), using Al-Cu alloy with ٠-٧ wt% Cu [٧].

(iii) Copper – Matrix Filler Metal Alloys

Naka and Arata[٥٠] fabricated non oxide (Silicon nitride, silicon carbide) ceramic joints using $Cu_{٥}$. $Ti_{٥}$. amorphous filler metal. Brazing of these ceramic to themselves was carried out in a vacuum of ٥×١٠^{-٥} torr and in the temperature range ٩٨٠-١٣٠٠°C. For a constant brazing time of ٣٠ minutes the silicon nitride/silicon nitride joint made by using $Cu_{٥}$. $Ti_{٥}$. showed a maximum strength of ١٨ $Kg/mm^{٢}$ (١٧٦.٥MPa) at ١١٠٠°C. The strength rapidly fell off to ١.٤ $Kg/mm^{٢}$ (١٣.٧٣ MPa) if the temperature was raised to ١٢٠٠°C. In the case of silicon carbide joints made using $Cu_{٥}$.$Ti_{٥}$., the joint exhibited a maximum strength of ٣.١ $Kg/mm^{٢}$ (٣٠.١ MPa) at ١٠٢٥°C.

X-Ray diffraction studies along with microprobe analysis of the fracture surface were used to determine the phases present at the joint interface.

Nicholas [٥١] patented several ternary alloy compositions. These alloys were evaluated for flow behavior as well as joint strength. They noted that the good flow in itself does not guarantee a strong joint, and he claimed strength up to ٤٠ MPa for joints fabricated using their alloys. The ternary systems investigated included Cu-Ti-Ag. For each of these systems isocontours of the contact angle for θ=١٠° and θ=٩٠° have been drawn in the ternary diagram representation. These are the results of extensive wetting tests, carried out on several oxide ceramics, at a temperature of ١٠٥٠°C. This is perhaps best demonstrated by comparing the result of Naka and Arata [٥٠] with those of Mizuhara et al. [٤٨].Both have used titanium as a reactive metal. In one case as much as ٣٠ at% of titanium (alloyed with pure copper)was necessary at a temperature as high as ١١٠٠ °C to obtain a contact angle of ٥°,whereas in other case only ٢ at.% of titanium(alloyed with Ag-Cu eutectic)was sufficient to cause complete wetting at a temperature less than ٨٥٠°C.In addition to other factors the wetting behavior is governed by alloy fluidity and superheat. Since the Ag-Cu eutectic melts at a much lower temperature(٧٨٠°C) than pure copper (١٠٨٣°C) it was possible to obtain a good flow at lower temperatures. It is also likely that the high fluidity of the eutectic based alloys coupled with a solidification pattern hence their wettability.This hypothesis is substantiated by the fact that the Ti-Cu eutectic around ٣٤ at.%Ti very close to the composition at which Naka and Arata found their binary alloys to flow well.

Moorhead and Keating [٥٢] have investigated the direct brazing of ceramics intended for adiabatic diesel engines. Their study was aimed at developing a suitable braze alloy to join heat engine ceramic to nodular cast iron for piston caps. The alloy Cu-٢٦Ag-٢٩Ti showed contact angles

($\theta < ١٥^{\circ}$) on alumina and Zirconia ceramics. The mechanical strength of $Al_{٢}O_{٣}$ joints was comparable to that of alumina. The zirconia brazment showed a flexure strength of ٣٠٠MPa, while the flexural strength of the zirconia (PSZ) itself was ٦٠٠MPa.

Another braze alloy (Cu-Au-Ni) systems with titanium additions showed high contact angles (up to ٩٠°) on alumina even at temperatures up to ١٥٠٠°C and were hence considered un suitable some of the Cu-Au-Ti alloys showed fairly high angles and did not adhere even at ١٥٠٠°C.

Efforts were also directed to understand the microstructual changes that occurred in the cast iron due to exposure to ١٠٠٠°C. A comparison of the microstructures in the cast iron revealed that the hardness of this alloy was unchanged after the brazing cycle. The pearlite nodules were finer and some trace of bainite were also seen. In general the pearlites plus the graphite microstructure desired for high cycle fatigue was pre served despite exposure to ١٠٠٠°C for ١٤-١٦ minutes. This is a significant result since it permits exposing the cast iron to high temperatures if necessary.

Standing and Nicholas [٥٣] conducted a meticulous and extensive wetting study on the Cu-Sn-Ti system, in the temperature regime of ١٠٥٠°C-١١٥٠°C on alumina and vitreous carbon. They used three different test temperatures of ١٠٥٠°C, ١١٠٠°C and ١١٥٠°C. They found that small amounts of titanium (٦-١٠٪) added to copper are sufficient to wet the ceramic ($\theta < ٩٠$) but high amounts of titanium, up to ٣٧.٥٪ are needed in binary alloys to cause the contact angle to reduce below ١٠°. Binary alloys of Cu-Sn exhibit very high contact angles up to ١٥٠° at ١٠٥٠°C. The ternary alloys of Sn, Ti. and Cu however wet very well on alumina. The Sn and Ti show a strong synergistic effect in reducing the contact angle. In fact the Cu-٧٩.٥٪, Sn-٩.٩% and Ti-١٠.٦٪ alloy shows an angle less than ١٠°. data on the carbon too. Some of their results are depicted in Fig. ٢-٥.

Metallographic examination of the interfaces of such samples revealed intermetallics at the interface of all alloys containing titanium but no intermetallics were seen for the alloys without titanium. Titanium confining alloys with contact angles of ١٤٢° showed a similar interfacial structure as that exhibited by alloys with angles less than ١٠°. The effect of tin additions on the wettability of the alloy was also not well understood.

The addition of tin to pure copper increases the contact angle, However, when tin is added to a binary Cu-Ti alloy it enhances the wettability considerably. The authors feel that in the ternary alloys segregation effects complicate the analysis. For example, it is known that the surface energy of pure tin is ٠.٤٨ $J/m^{٢}$, while that for copper is ١.٢٨ $J/m^{٢}$ at ١١٠٠°C. Hence, energetically it is

expected that in Sn-Cu alloys, Sn will segregate to the surfaces. On this basis they suggest the addition of other elements with surface energies lower than copper as possible agents for improving wetting.

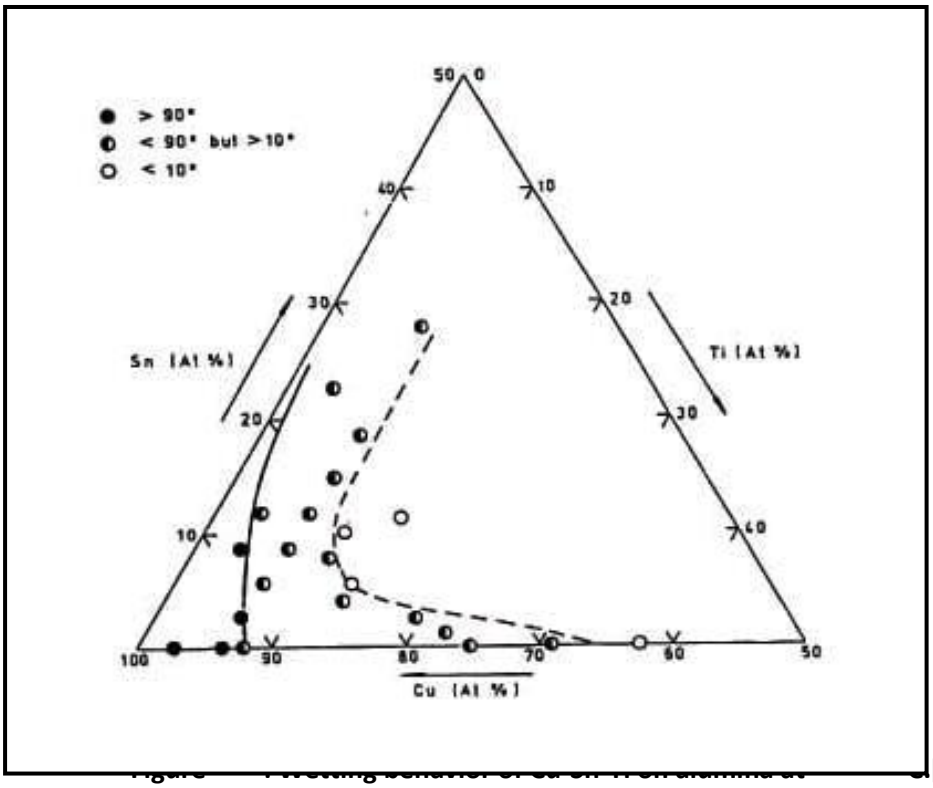

[٥٣]

Zhenfeng Zhou *et al*[٥٤]*.,* studied the interfacial reaction and strength in the joining Si_3N_4/Si_3N_4 with newly developed CuNiTiB brazing alloy at ١٣٥٣K for ١٠min. The shear strength with powdered $Cu_{٦٨}$-$Ni_{١٠}$-$Ti_{٢١}$-$B_١$ brazing alloy of joint reach ٢٣٣ MPa.With rapidly solidified foils of the brazing alloy, the three-point bend strength of the joint is raised to ٤٠٦MPa at room temperature, and this value remained steady at ٧٢٣K. The interfacial reactions were studied of the joint and its effects on the joint strength. The lattice matching between Si_3N_4 and Ti_5Si_5 is better than that between Si_3N_4 and TiN. So the formation of Ti_5Si_3 than TiN at the interfaces is favorable to the joint strength. Ni element adding to Cu-Ti alloy can weaken the activity of Ti in the alloy[٥٤], which is favorable to decrease the thickness of interfacial reaction layer and in the result the joint strength is increased. Adding a small amount of B in the new alloy can decrease its liquids temperature.

Fadhel A.H. [٣] investigated the joining alumina to alumina using a single stage brazing. A brazing matrix study was carried out on several alloys Cu-Ti, Cu-Zr and the eutectic Ag-Cu-Ti system. These alloys were prepared in two type: true-filler metal alloy, and past-filler metal alloy.

Double shear tests were performed on the various interfaces. The maximum strength ٤٢.٢٥ MPa was showed when used Ag-Cu-Ti as a past form. Cu-Ti past-filler also was showed a high joint strength, in comparison with eutectic Ag-Cu-Ti system.

X-ray and SEM analysis of the joint interfaces reveled two phases of the brazing region: phase I ($Cu_2(Al, Ti)_4O$) or (ZrO_2) responsible for interface bonding phase II (CuTi structure) or (Cu+Zr) works as a matrix for bonding phase.

٢.٣ Ceramic-Copper Joining

Bonding between ceramic and copper can be obtained by the "diffusion bonding" process "Cu-Cu_2O eutectic bonding" process and "brazing" process:

٢.٣.١ Ceramic-to Copper Diffusion bonding

M.Courbiere *et al* [٥٥] studied the solid state bonding between copper and alumina using ٠.٢mm thick (OFHC) of Cu disk and ٨mm thick of ٩٩.٧wt % Al_2O_3 ceramic disks both of ٥mm diameter. Optimum shear strength values of ٥٠ MPa were obtained after bonding at ١٠٠٠°C/ ٦MPa / ٢h in an argon atmosphere. The mean roughness *Ra* of the ceramic surfaces of these Al_2O_3/Cu/Al_2O_3 joints was ٠.٣μm. A distinct influence of the roughness of the alumina surface on the bond strength and the fracture behavior of the joints was observed. High Ra values of ٠.٦ and ١ μm produced by grinding with diamond of grain size ٤٠ and ١٥٠μm, respectively, lead to the low strength value of ٢٠ and ١٥ MPa. The reduction in strength was caused by the introduction of flaws into the ceramic interface region and by pull-out of grains. Extensive void formation was found at the copper side of the interface fracture of joints manufactured from well –polished (*Ra*=٠.٠٥ μm) ceramic pieces. The effect was thought to be caused by gas evaluation. TEM studies revealed that very small Cu_2O particles were dispersed in copper only a ٠.١μm layer of microcrystalline alumina but no reaction layers was detected at the metal/ ceramic interface. In another set of experiments copper was preoxidized before bonding by annealing at ١٠٠٠°C in a low oxygen atmosphere to produce ٠.٧ and ٢.٢μm Cu_2O layers on Cu.Generally the bond strength of preoxidized Cu was lower than that of nonoxidized Cu and decreased after a maximum at ١ or ٢h with increasing bonding time. Fractographic studies revealed the extence of ٣ different bonding zones. The inner zone III contained $CuAlO_2$ at the interface after ٢h bonding time, after ٦h it was disappeared and was substituted by microcrystalline Al_2O_3 layer of about the same thickness. Zone III was under the normal compression stress during bonding. The middle zone II is a zone of adhesion. It had an

annular shape. The copper was plastically deformed during welding in this region of high shear stresses. The outer zone I not subjected to high stresses during bonding showed variable adhesion and was in contact with the furnace atmosphere. $CuAlO_2$

which was formed at the beginning of the bonding treatment was destabilized in favor of Al_2O_3 and Cu_2O by diffusion of Oxygen. This was correlated to the observed decrease in bond strength.

Cu/Al_2O_3 joints were studied with respect to their fracture toughness and the influence of the bonded area and interfacial impurities on the bonding behavior $Al_2O_3/Cu/Al_2O_3$ joints were fabricated from an alumina ceramic of grain size ١٨μm (mean intercept length) cut to dimensions ١١.٦.١٫٥ mm^3 containing ٣٠٠ wt. ppm Mg, ٢٥ ppm K, ٢٠ ppm Na, and ٦ ppm Ca and high purity ٣٠μm thick polycrystalline Cu foils containing ٢٠wt. Ppm Ag as the main impurity [٥٦].Bonding was carried out in the temperature range ٨٥٠ to ١٠٥٠°C for ١٠min under a mechanical pressure of ٢٠ MPa. The bonding atmosphere was a purified gas mixture of ٢٥/٧٥ Vol% H_2/N_2 which contained less than ١ vol. Ppm H_2O. The fracture toughness of the joints was determined by double cantilever beam (DCB) tests. The obtained fracture toughness data K_{Ic} were ١.٩, ٣.٧, ٤.٣, ٤.٢ and ٤.٥ MPa. $m^{1/2}$ for Joints bonded at ٨٥٠,٩٠٠, ٩٥٠, ١٠٠٠ and ١٠٥٠°C, respectively. The fracture toughness of the alumina ceramic was ٣.٢ $MPa.m^{1/2}$.

Arata *et al* [٥٧] studied the diffusion bonding between alumina and Cu-٤٪ Ti alloy using ٥mm thick ceramic disks of ١٥mm diameter and ٠.٦ mm thick metal disks of ٦ mm diameters. Optimum bonding was obtained after welding of sandwich-like configurations ceramic /metal/ ceramic at ٨٠٠°C/ ٢٠min/ ٥٠MPa in a vacuum of ٧×١٠^{-٥}m bar. The tensile bond strength was ٤٥ MPa from a joint fabricated from ٩٩.٦wt% alumina and Cu-٤ wt% Ti however, the bond strength of Al_2O_3 / Cu/Al_2O_3 joint was only ٢٠MPa.

C.Scheu *et al.*, [٥٨] have studied the effect of annealing at ١٠٠٠°C at oxygen partial pressures of ٠.٠٢ or ٣٢Pa of diffusion bonding between $Cu-Al_2O_3$. The advantages of the solid-state bonding technique are the production of an interface free of reaction phases and the presence of a well-defined interface state before further annealing. At the low oxygen partial pressure, only the $CuAlO_2$ is a thermodynamically stable reaction phase as determined from the phase stability diagram calculated by Rogers et al [٥٨] for the ternary Cu-Al-O system. Annealing in the higher oxygen partial pressure can additionally lead to the formation of Cu_2O. the expected changes of adhesion was investigated by contact angle measurements in solid state. XRD and SEM investigations of the fractured samples revealed that annealing under both oxygen partial pressures resulted in the

formation of $CuAlO_2$ layer at the interface between Cu and αAl_2O_3. the reaction layer is not continuous and separated by many pores. The interfacial pores formed in the as- bonded and the annealed specimen, which were used to measure the contact angle. For the as-bonded sample, a contact angle of ١٣٠±٧° was determined. A detailed study of more than ٢٠ pores revealed that the contact angle varied between ١٠٧° and ١٤١°. For the samples annealed in $P(O_2)$=٠.٠٢ or ٣٢Pa, the contact angle between Cu and the $CuAlO_2$ layer varied between ٩٩° and ١١٠°.

The authors observed a needles of $CuAlO_2$ for the higher oxygen partial pressure, $CuAlO_2$ needles, which were several millimeters long and up to ١μm high.

C.Beraud et al.[٥٩[studied copper to alumina bonding by solid state .The temperature of bonding is varied from ٧٠٠ to ١٠٠٠ ºC ,the pressure applied in the range ١ to ٨ MPa and the holding time is varied from ٣٠min to ٦h.Fig ٢-٦(a) shows the effect of temperature on the strength of bonding and Fig.٢-٦(b) shows the effect of temperature on the percentage of adherent zones.

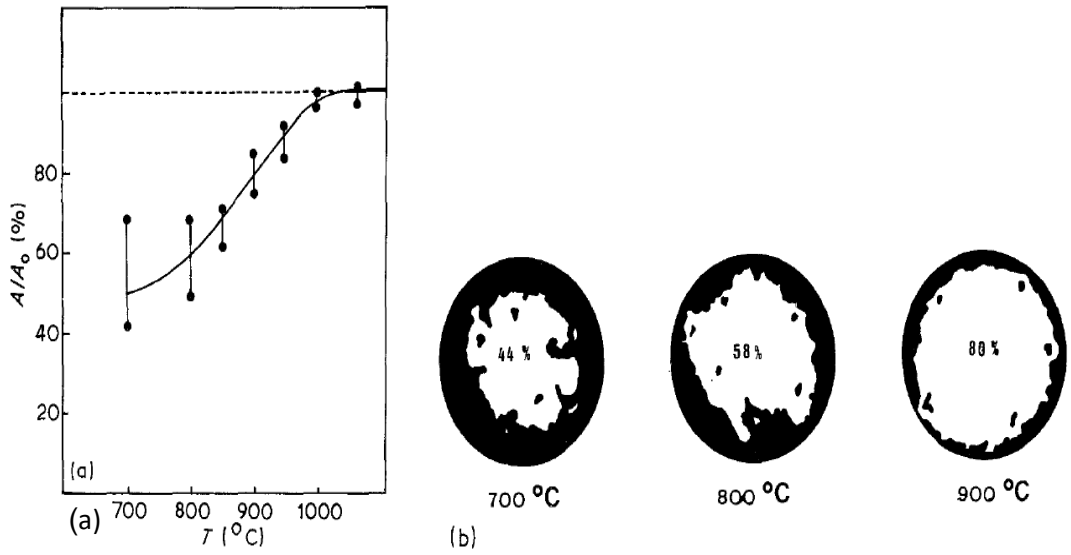

Contact area for different temperatures (adherent zones are white)[٥٩].

٢.٣.٢ Cu-Cu_2O Eutectic Bonding

C. Beraud *et al.,* [٥٩] studied the bonding between copper and alumina by the liquid phase bonding process. They used a copper-oxygen eutectic system for a composition of ٠.٣٩ wt % of oxygen. The maximum wettability seems to be reached at the eutectic composition[٦٠]. This is in accordance with the fact that the wettability of alumina by liquid copper is strongly increased by the presence of oxygen [٦١]. The melting temperature of the eutectic (١٠٦٥°C) lies slightly below the

melting temperature of copper (١٠٨٣°C). In the temperature range of ١٠٦٥ to ١٠٨٣°C a liquid phase appears at the Cu_2O-Cu interface. This thin molten film produces an intimate contact between copper and alumina and generates, after cooling, a strong bond between the two materials as shown in Fig.٢-٧

Figure ٢-٧: Evaluation angle ϴ for liquid copper upon alumina as a function of oxygen content in the copper drop after cooling[٦٠]

The thickness of Cu_2O films produced by oxidized under low oxygen pressure (10^{-1} torr) at ١٠٠٠°C is varied from ٠.٣ to ٧٠μm. The bonding temperature is ١٠٧٠°C and the time of bonding is ٢ min. The optimal strength (١٤٠ MPa) is obtained for Cu_2O thickness laying between ٣ and ١٠μm. Fracture strength, i.e. adhesion, depends on the amount of liquid eutectic and consequently on the Cu_2O layer thickness. Between ٣ and ١٠μm thickness, the eutectic phase comes into intimate contact with alumina and rupture occurs at the alumina- eutectic interface or in the eutectic phase. Beyond a Cu_2O thickness of ١٠μm decrease in tensile strength is observed as a consequence of the numerous large pores located at the interface. The authors also studied the fracture toughness of Cu-Al_2O_3 bonds, and the maximum fracture toughness (K_{Ic}) were obtained similar to that one of bulk alumina (٣.٧ MPa $m^{1/2}$). The measured K_{Ic} values decrease if the Cu_2O layer is thinner than ٣μm or thicker than ١٠μm. The authors offered an explanation for the pores fracture toughness of a thin Cu_2O layer that the fracture energy of the interface low because insufficient eutectic is formed to wet all the ceramic surface and with thicker Cu_2O layer, the brittleness of the bond is increased and the crack resistance behavior of the interface is considerably reduced compared to that of the bulk alumina.

In a similar study [٥٨,٦٣-٦٤,٦٧] perform on eutectic – bonded samples where a liquid Cu_2O layer on a pre-oxidized Cu surface was in contact with Al_2O_3 during the bonding procedure. It was found that, because of the high oxygen content in the molten layer, reaction phases could easily form possible phases in the Cu-Al-O system were the ternary aluminates $CuAlO_2$ and $CuAl_2O_4$ or the binary oxides Cu_2O and CuO [٥٨, ٦٥-٦٦].

٢.٣.٣ Ceramic-to Copper Brazing

M. Naka *et al.,* [٦٨] studied the brazing of alumina to copper using a ٥٠ at% Cu- ٥٠ at% Ti filler alloy. The reaction layer consists of a copper-rich phase with some titanium, together with the oxides TiO_x and $(Al, Ti)_2O_3$. several oxide compositions are possible such as the formation of TiO(γ-

TiO, β-TiO and β-$Ti_{1-x}O$), Ti_2O_3, Ti_3O_5 and TiO_2.The latter form is the most stable one. The possible chemical reactions together with their free energy of formation are summarized in Table ٢.٣.

In a similar study Naka et al., used $Cu_{0.}$ $Ti_{0.}$ amorphous filler metal to optimize the joining conditions between alumina to copper and alumina to kovar [٦٩-٧٠] The results from mechanical testing of elevated temperatures have been plotted in Fig. ٢-٨.

Table ٢.٣: Possible reactions between titanium-containing fillers and oxide ceramics (standard Gibbs energies calculated from data given in [٧,٧١- ٧٢].

Reaction	Free energy (kJ mol^{-1})
٢ Ti(s) +O_2(g) = ٢TiO (s)	$\Delta G°$=-١٠٢٣+٠.١٧٨T
٤/٣ Ti(s) +O_2(g) = ٢/٣Ti_2O_3 (s)	$\Delta G°$= - ١٠٠١ + ٠.١٧٢T
٦/٥ Ti(s) +O_2(g) = ٢/٥Ti_3O_5 (s)	$\Delta G°$= - ٩٧٥ + ٠.١٧١T
Ti(s) +O_2(g) = TiO_2 (s)	$\Delta G°$= - ٩١٤ + ٠.١٧٥T

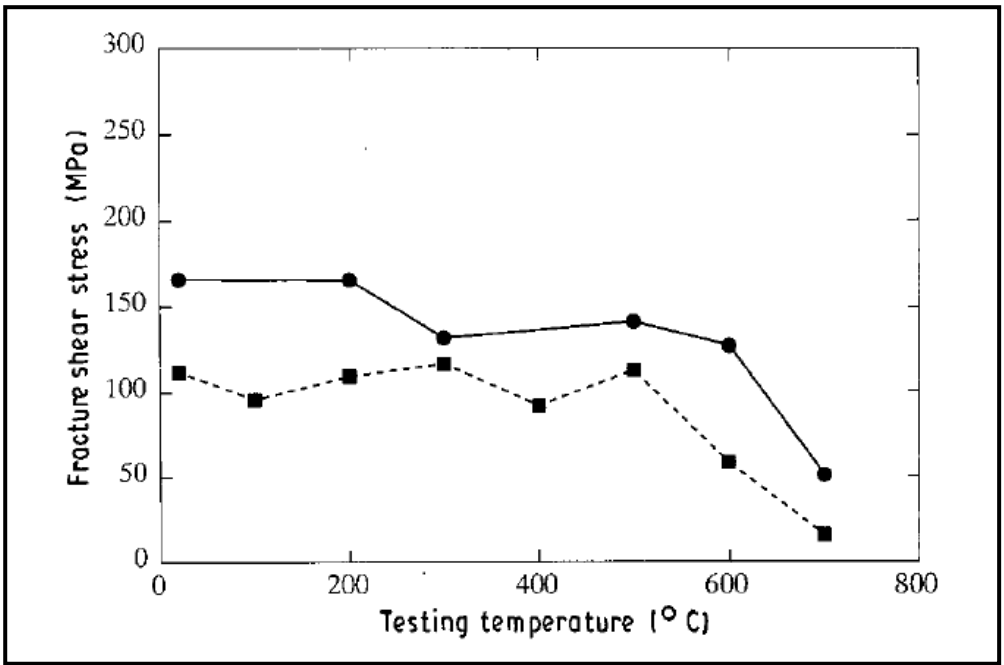

Figure ٢.٨: Effect of testing temperature on fracture shear stress of Al_2O_3-metal joints brazed with ٥٠ at % Cu – ٥٠ at % Ti filler alloy in vacuum for ٣٠ min; brazing temperature (■)

١٠٢٥°C for copper (after Naka *et al.* [٦٩]) and (●) ١١٥٠°C for Kovar (after Naka *et al.,* [٦٨]).

In the former case, the room – temperature strength level is maintained at temperatures below ٥٠٠ and ٦٠٠°C for copper and kovar (Fe-٢٩ wt% Ni- ١٧ wt% Co alloy), respectively. Beyond these temperatures, the fracture shear stress has been significantly reduced. It should be noted that the maximum room-temperature bond strength of alumina-copper joints occurs for a brazing alloy titanium content of ٣٠-٤٠Wt% [٧٣], which is in agreement with the level required to obtain a minimum wetting angle. It is therefore implied that the elevated-temperature strength of alumina-copper joints is mainly controlled by metal properties, since alumina normally tolerate exposure to high temperature before strength redaction occurs.

Kuzumaki *et al.,* [٧٣] studied the effect of cobalt and niobium to Ag-Cu-Ti alloy filler metal to joint copper to aluminum nitride. They found that small amount of cobalt(٥wt%) and niobium(٥wt%) added to filler metal are sufficient to improve the joint strength by ٣٠ MPa.They claimed that cobalt exhibited same behavior as titanium on brazing of ceramic to copper.

Cobalt is usually add as a binder to carbides powder of tungsten ,tantalum and titanium when manufacture cutting tool by powder metallurgy and improve the wetting of powder by reducing the surface energy and forms a eutectic with the carbides at elevated temperature and this eutectic becomes the cemented material[٧٤].Wetting in WC-Co system is controlled by the cobalt at the intergrainular spaces in the WC. Cobalt is soluble in copper ,thus, molten copper on WC-Co materials will have in a manner similar to a "reactive metal" in that it will dissolve cobalt and flow over the carbide. The data in literature indicates that better wetting of carbide is obtained at about ٥-٦wt%Co(see Fig.٢-٩) level and if the cobalt exceed this limit may be attributed to depletion of titanium from the matrix and forms intermetallic $Ti_٢Co$ and TiCo phases.[٧٥-٧٨].

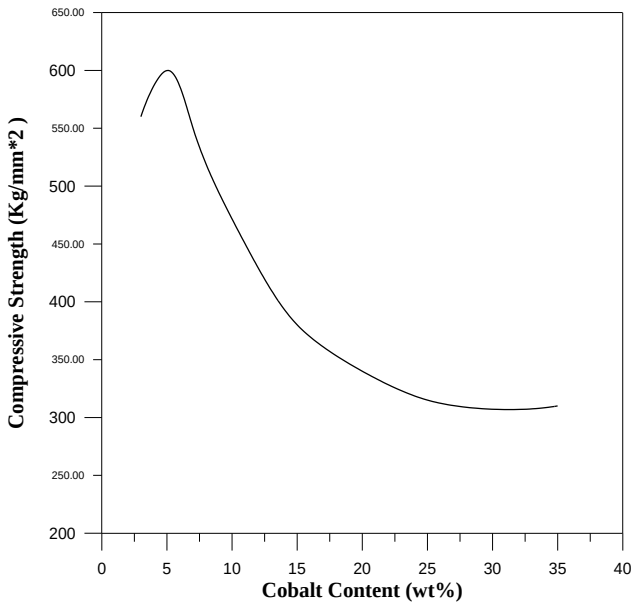

Figure ٢.٩: Effect of cobalt on the compressive strength of WC-Co compositions [٧٦].

W. C. Lee and O. Y. Kwon [٧٩] investigated the effect of adherent metals on the microstructure and microchemistry of reaction product formed at the Al_2O_3/ filler metal interface for the joint brazed Al_2O_3/Cu with three types of brazing alloys: Cu – ٣٤.٨ Ag – ٦.٢ Ti, Cu-٣٠.٦Ag-٥.٥Ti-١١.٩Al and Cu-٣٣.٧Ag-٦.١Ti-٣.٠Sn in atomic percentage.

They observed that the reaction products of Al_2O_3/Cu joint showed a layered structure consisting of TiO and Cu_2Ti_4O. The TiO compound was formed by redox reaction between Al_2O_3 and titanium, whereas Cu_2Ti_4O compounds formed by solid-state reaction between TiO and brazing alloy.

Naka *et al*[٨٠] studied the effect of titanium precoating on wetting and joining of copper to silicon carbide ,they showed that maximum strength of the joint at ١٠μm of titanium thickness. and the excess amounts of carbide and silicide cause the degradation of copper near the interface of Cu/ SiC, though the formation of compounds accelerates the wetting of copper on Sic. This is attributable to the maximum of joining strength of copper against SiC.

Graphite is an important material in nuclear industry .In the fusion reactors graphite used as a first wall material to minimize impurities in the reactor. The graphite tiles used there face enormous heat load. Unless there is an efficient heat removal mechanism in place, temperatures rise beyond tolerable levels. The practice is to attach water cooled sheets of copper or copper alloy to graphite tiles. It is imperative that thermal contact between graphite and copper be very good in order to reduce thermal resistance. This can be achieved only by brazing the two[٨١].

Naka and Hafez [٨٢] studied the effect of ultrasonic wave and brazing temperature on the properties of the braze joint between alumina and copper using Zn-Al alloys as a filler metal. The alumina was metallized by applying an ultrasonic wave in a Zn-Al braze bath, then the metallized alumina was brazed with copper using the same filler alloy. The ultrasonic waves improved the wetting in the molten Zn-Al bath by accelerating the removal of bubbles from the interface between alumina and the filler, and this was reflected in improved joint strength. The brazing filler were Zn-Al alloys, containing Al content from ٠ up to ١٠ mass %. The brazing temperature were ٦٧٣, ٧٢٣ and ٧٧٣ K. The applying time of ultrasonic waves from ٠ to ٩٠ second promoted the wetting of filler alloy against alumina and raises the joint strength. The maximum strength (٨٥ MPa was obtained at the temperature ٧٧٣K for ٤٠ sec.).

Chapter ٣

The Difficulties for

Joining Ceramic to Metal

٣.١ Introduction

The challenges associated with ceramic metal joining can be classified as either chemical or mechanical in nature. Significant advances have been made in the field of chemical control. The initial wettability limitation has been overcome through the use of active metals. While a qualitative understanding of the formation of reaction products and their influence on joint strength has begun. A through understanding of the energetics , interface thermodynamic , structure and properties of this interface is crucial to control of the joining process. Hence, a study of wetting behavior , residual stresses are essential to the braze alloy designer.

٣-٢ Interface Thermodynamics

The fundamental role in theoretical understanding of wetting and adhesion phenomena belongs to thermodynamic analysis. In particular, the difference between the wetting and non-wetting behavior, or the value of the wetting angle, is essentially determined by the relative values of different thermodynamic quantities, like interface energies, work of adhesion , and surface energies.

In general an interface in a material represents a location where the atoms are coordinated to a lesser extent than the bulk atoms due to a large number of unshared bonds. Consequently these atoms are in a higher energy state than the bulk atoms, this leads to the concept of a surface energy associated with any surface.

The fundamental understanding of the structure and characteristics of a ceramic-metal interface is essential to introduce the main interface thermodynamic quantities.

٣.٢.١ Definition of Interface Free Energy

The most fundamental property in a thermodynamic description of an interface is its free energy per unit area, γ [٨٣-٨٤]. This quantity is best defined by considering a system that consists of two bulk phases, A and B which are in contact along a planar internal interface. The system is growing in a container under some given equilibrium conditions by the accretion of atoms from suitable reservoirs. The growing interface system and the reservoirs are maintained at constant temperature, *T*, Pressure, *P*, and chemical potential , μ_i of each of the components. It is also assumed that the size of the system in all dimensions is much larger than the width of the interface regions. Then, in accordance with the first and second laws of thermodynamics, the change in the internal energy of the system, *E*, due to the accretion can be expressed as [٨٣]

$$dE = TdS - PdV + \sum_{i=1}^{c} \mu_i dN_i + \gamma dA,..... \qquad (٣\text{-}١)$$

where *S* is the entropy, *V* the volume, N_i the amount of component i, c the number of components, and A the area of the planar surface. Compared to the corresponding expression for a bulk system, Eq.(٣-١) contains an extra term, γdA which describes the increase in the internal energy of the system associated with the increase in the area of the interface. Equation (٣-١١) implies

$$\gamma = \left[\frac{\partial E}{\partial A}\right]_{S,V,N_i} \qquad (٣\text{-}٢)$$

Thus, the interface free energy γ can be defined as the increase in the internal energy of the entire system per unit increase in interface area at constant *S* and *V* at the system under closed conditions, i.e. at constant N_i.

The state of a thermodynamic system under different thermodynamic constraints can be found by minimizing an appropriate thermodynamic variable. The most important examples of such thermodynamic variables are the Helmholtz free energy[٨٣],

$$F = E - TS, \qquad (٣\text{-}٣)$$

for a closed system at constant T and V, the Gibbs free energy,

$$G = E + PV - TS, \qquad (٣\text{-}٤)$$

For a closed system at constant T and P, and the grand potential,

$$\Omega = \mathrm{E} - \mathrm{T}S - \sum_{i=1}^{c} \mu_i \mathrm{N}_i \qquad \textbf{(٣-٥)}$$

which is used to describe an open system under conditions of constant *T*, *V*, and μ_i.

With those definitions and Eq.(٣-١) the interface free energy can also be defined as

$$\gamma = \left[\frac{\partial F}{\partial A}\right]_{T,V,N_i} \qquad \textbf{(٣-٦)}$$

$$\gamma = \left[\frac{\partial G}{\partial A}\right]_{T,P,N_i} \qquad \textbf{(٣-٧)}$$

$$\gamma = \left[\frac{\partial \Omega}{\partial A}\right]_{T,V,\mu_i} \qquad \textbf{(٣-٨)}$$

There is one more interesting form of an interface free energy definition. By integration Eq.(٣-١).

$$E = TS - PV + \sum_{i=1}^{c} \mu_i N_i + \gamma A, \ldots\ldots \qquad \textbf{(٣-٩)}$$

and using Eq.(٣-٤) , one can express γ as

$$\gamma = \frac{1}{A}\left[G - \sum_{i=1}^{c} \mu_i N_i\right] \qquad \textbf{(٣-١٠)}$$

here, the quantity $\sum_{i=1}^{c} \mu_i N_i$ can be identified as the total Gibbs free energy which the homogenous A and B bulk phases would have together if they were made up of the same amounts of the components at the same chemical potentials. Thus, the interface free energy γ is the excess Gibbs free energy of the entire system per unit interface area due to the presence of the interface.

If no thermal motion of atoms is included, *T*= ٠. Moreover, in view of the relatively low compressibility of the solids and liquids in the context of the present work it is also reasonable to neglect the contribution of the *PV* term in Eq.(٣-٤). Thus, Eq.(٣-٤) gives.

$$G \cong E \qquad \textbf{(٣-١١)}$$

Under these assumptions , the interface free energy, or simply interface, can be viewed as the work per unit area required to form the two interfaces *A/B* and *B/A* from the two bulk crystals *A* and *B* [٨٤], as illustrated in Fig. ٣-١.

$$\gamma = \gamma_{A/B} = \left(E_{A/B} - E_A^{(bulk)} - E_B^{bulk}\right) / A \qquad \textbf{(٣-١٢)}$$

Here $E_{A/B}$ is the total energy of the *A/B* interface system, and $E_A^{(bulk)}$, $E_B^{(bulk)}$ are the bulk total energies per each of the A and B half crystal, i.e. the total energy per structural unit of the corresponding bulk crystal multiplied by the number of the structural units in the corresponding half-crystal. The interface energy shows how much weaker the bonding at the interface is than in the *A* and *B* bulk materials.

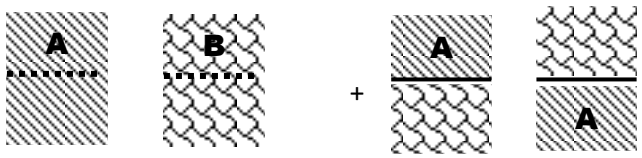

Figure ٣-١: A schematic diagram illustrating the definition of the interface energy[٨٣].

٣.٢.٢ Thermodynamics of Wetting Contact Angle and Work of Adhesion

The thermodynamic description of interface systems introduced in the previous section can be applied to the situation of wetting experiments. A typical situation of sessile drop wetting experiments, with a metal drop on a ceramic surface, is schematically shown in Fig. ٣-٢. The contact angle θ characterizes the degree of wettability of a given ceramic by a given metal: θ =٩٠° is considered as a boundary between the wetting (θ <٩٠°) and non-wetting (θ >٩٠°) behaviors. The smaller the angle θ the better is the wetting. In addition to characterizing wettability itself, wetting experiments are practically the only feasible way to study interface thermodynamics (energetics) in metal-ceramic systems[٧-٨٣].

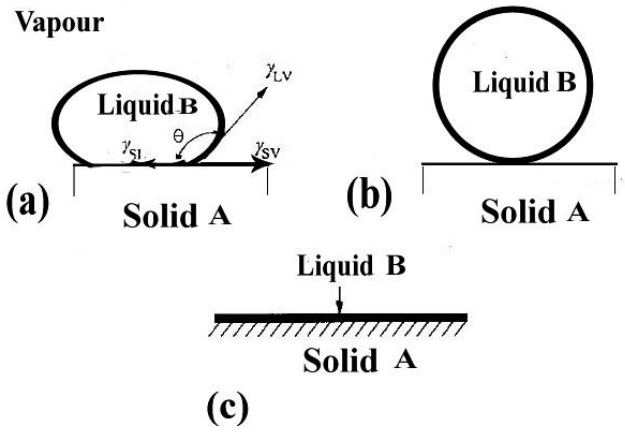

Figure ٣-٢: Principles of wetting(a)definition of wetting angle ɵ by surface-tension balance for a liquid drop(B)on a solid surface(A)(schematic),(b)no wetting and(c)complete wetting[٧].

Under thermodynamic equilibrium and steady state conditions, the contact angle θ is determined by the Young equation:

$$\cos\theta = \frac{\left(\sigma_A - \gamma_{A/B}\right)}{\sigma_B} \qquad (٣\text{-}١٣)$$

Here $\gamma_{A/B}$, σ_A, and σ_B are the interface free energy values for the solid-liquid A/B, solid-vapor, and liquid – vapor interfaces, respectively. The quantities σ_A and σ_B are at the same time the surface energies of solid A and liquid B, respectively. A decrease in the contact angle, on the one hand, lowers the free energy of the system. This is due to the fact that part of the substrate free surface is replaced by liquid-solid interface area, which normally has a lower energy. On the other hand, this lowering of free energy is partially compensated for by the energy of the increasing area of the free liquid surface (liquid-vapor interface). The young equation simply states the condition of a balance between those two opposite contribution, i.e. the condition of a free energy minimum[٨٣].

An interesting and important form of the contact angle expression (Eq.٣-١٣) can be obtained by introducing one more important quantity, the work of adhesion, W_{ad}, this quantity is defined as the reversible free energy changes for making free surfaces from interfaces[٨٥], whereby the surfaces are in equilibrium with the solid and gaseous components. The work of adhesion W_{ad} is connected to the corresponding interface and surface energies via the Dupré equation[٧-٨٣]:

$$W_{ad} = \sigma_A + \sigma_B - \gamma_{A/B} \qquad (٣\text{-}١٤)$$

combination of Eqs. (٣-١٣) and (٣-١٤) leads to the young-Dupré equation

$W_{ad} = \sigma_B (1+\cos\theta)$ **(٣-١٥)**

With this equation, the measured wetting angle directly gives the ratio of the interface adhesion work W_{ad} and the liquid metal surface energy σ_B.

The Young-Dupré equation (٣-١٥) plays an important role in the analysis of wetting experiments. The contact angle θ is what is actually measured in the sessile drop wetting experiments. The liquid surface energy at a given temperature is typically known from a separate experiment the same study, or from the available data from other experimental work. The work of adhesion W_{ad} is practically the only interface thermodynamics (energetics) quantity that can be directly extracted from the wetting experiments. A reliable measurement of the solid surface energy σ_A is a very problematic task, making it almost impossible to get any good estimates of a solid- liquid or solid-solid interface energies $\gamma_{A/B}$ with Eq.(٣-١٤)[٨٣].

٣.٢.٣ Ideal Work of Separation as Measure of Interface Adhesion Strength

An other fundamental quantity in the interface thermodynamics is the ideal work of separation W_{sep}, which is defined as the reversible work needed to separate the interface into two free surfaces in a though experiment, whereby plastic and diffusional degrees of freedom are suppressed. The ideal work of separation can be expressed by a modified Dupré equation[٨٣-٨٥]:

$$W_{sep} = \sigma'_A + \sigma'_B - \gamma_{A/B} \qquad \textbf{(٣-١٦)}$$

The difference from the Dupré equation (٣-١٤) is that the surface energies σ_A and σ_B are now replaced by the instantaneous values of surface energies before any plastic processes, like dislocation motion, or diffusional processes of chemical equilibration, like surface segregation or surface contamination, take place. Due to such dissipative processes, the energy needed in a real cleavage experiment will always exceed W_{sep}. Yet, it is still a very useful quantity to characterize interface mechanical strength.

As discussed by Finnis [٨٥] while it is very problematic to directly calculated the contact angle or the work of adhesion Eq. (١٤), it is a much more manageable task to calculate the ideal work of separation W_{sep}, by comparing the total energy of interface system with the total energy of

the corresponding system in which the interface is cleaved, leaving two free surface Fig. ٣-٣. Due to such calculational difficulties, the theoretical analysis of wetting in the appended papers assumes

$$W_{ad} \cong W_{sep.} \qquad \textbf{(٣-١٧)}$$

where $W_{sep.}$ Is calculated without any explicit inclusion of thermal motion, i.e. at T=٠, as

$$W_{sep.} = W_{A/B} = \left(E_{A|} + E_{|B} - E_{A/B}\right)/A \qquad \textbf{(٣-١٨)}$$

Here $E_{A|}$ and $E_{|B}$ are the total energies of the separated half-crystals.

Figure ٣-٣: Illustration for the definition of the work of separation[٨٣].

٣.٣ Chemical Nature of Ceramic-Metal Joining

Reactivity is the primary chemical consideration when joining ceramic-to-metal. The lack of reactivity manifests itself in the from of non-wettability, i.e., when one material fails to adequately cover the surface of another. Generally joint strength is proportional to coverage, making adequate wettability essential. On the other hand, excessive reactivity can lead to the formation of porosity of brittle intermetallics. For systems with widely disparate material properties, this find balance can be difficult to achieve.

The structures at metal-ceramic interfaces are classified into the following four types[٨٦'٨٧] as illustrated in Fig. ٣-٤

a-Non-reactive and non-penetrative,

b-Penetrative

c-Reactive, and

d-Diffusive

The interfaces which belong to type (a) are microscopically planar and are coherent (epitaxial) or incoherent, A coherent interface has been observed in some joints, such as niobium/

alumina, platinum／ alumina and platinum／cubic zirconia systems. The interfaces which belong to type (b) are mainly made by penetration of metal into ceramic during joining under a high pressure at high temperatures, in particular, when the composite of mixture of both powders of the metals and ceramic is used as interlayer to decreases thermal stress coming from the thermal expansion mismatch between the metal and the ceramic.

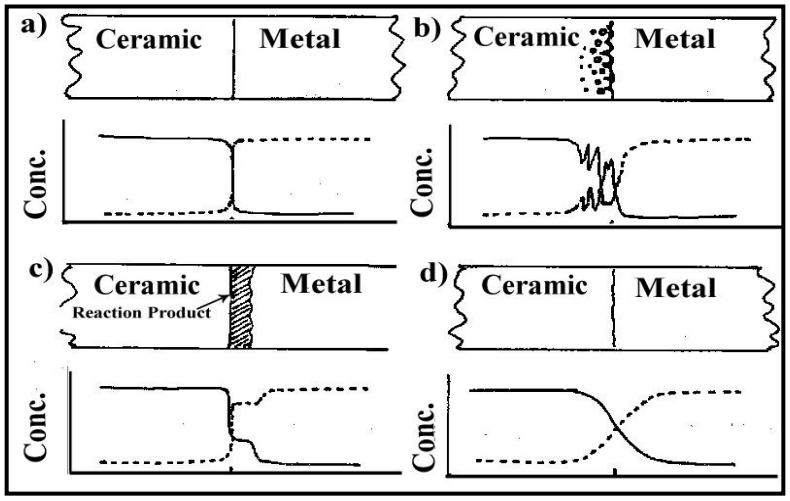

Fig. ٣-٤: Four types showing metal-ceramic interfacial structures and distribution profiles of species between metal and ceramic(a)Non-reactive and non-penetrative, (b)Penetrative (c)- Reactive, and (d)- Diffusive[٨٦].

The penetrative interface is produced with ease. Therefore, the interface is complicated and not planar. The majority of metal-ceramic joints reacts chemically at the interfaces, belonging to type (c). In some couples many kind of compounds are formed at the interface[٨٦].

Structural ceramics are among the most stable compounds known and as a result are very difficult to wet. This thermodynamic limitation can be overcome through the kinetics of chemical reactivity. If the interface material contains an element which forms a more stable oxide than the solid oxide on which the liquid metal is held, wetting or spreading of the liquid occurs [٨٧]. For example, when bonding alumina and steel, active metals such as titanium or zirconium are often used in the form of vapor-deposited coating or as a component within the braze alloy. Because titanium has a higher affinity for oxygen than aluminum, it effectively wets the ceramic while sharing enough metallic similarity with the steel to effectively join with it as well[٨٧].

Chemical reactions between materials during joining have a significant influence on the strength of joints. Unfortunately, this is about the most definitive statement that can be made about

the effect of reactivity. There are nearly as many sources in the literature stating reactivity improves strength as those which refute it [٢,٦٨,٨٧].In general , reactivity on the atomic scale improves bonding, while the formation of bulk amounts of porous ceramics or brittle intermetallics almost always proves deleterious.

These various issues can be more clearly understood by examining a molybdenum: silicon carbide braze joint using a copper interlayer with titanium as a metallization layer. As the amount of titanium increases by increasing the thickness of the sputtered metallization layer, the wettability of the ceramic increases. At a critical thickness, the wettability of the ceramic reaches a maximum. While the titanium reacts with the ceramic, it also diffuses into the copper, creating the brittle Ti_xCu intermetallic.These competing reactions create a strength maximum for the overall joining system. Fig. ٣-٥. the negative effects of reactivity are further illustrated by a diffusion bonded silicon nitride / silicon nitride joint using an aluminum interlayer. For a given temperature, a certain amount of time is required for adequate wettability between interlayer and the ceramic. After an extended period of time, the formation of deleterious reaction products being and joint strength is compromised- Fig. ٣.٦ [٨].

The challenge is to develop an interlayer system of prescribed reactivity which effectively wets both materials while keeping the production of reaction products to a minimum. This is a rather complicated exercise as a dissimilar joining systems with two separate components and an interlayer may form up to nine distinct phases. An example of this is shown in Table ٣.١. where reaction products found in various metal: ceramic joints are listed [٨٦].Given the complexity of this analysis, alloy systems have been designed by using computational thermodynamics, which produce strong joints with relatively little dependence on bonding time .

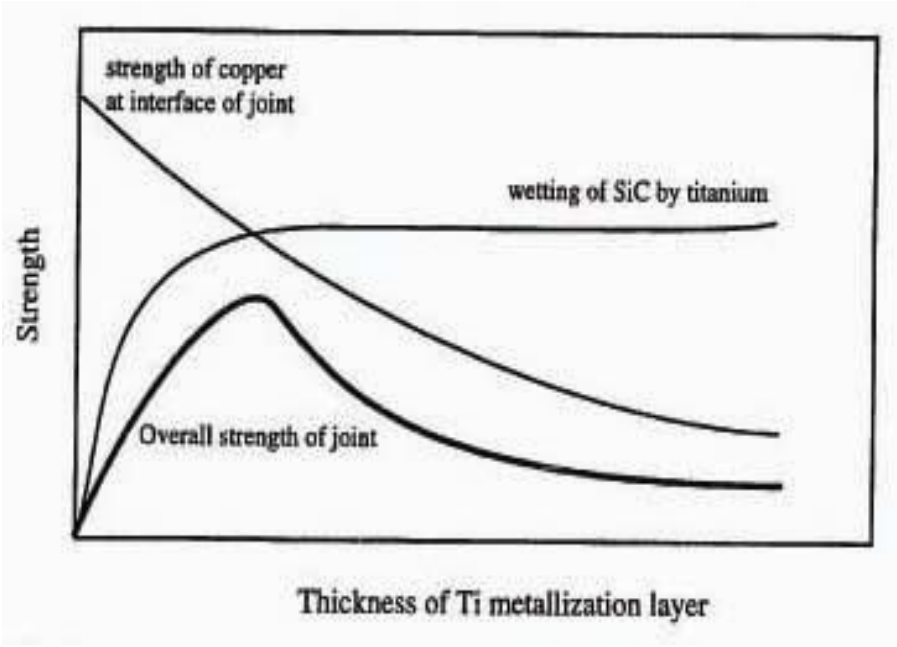

Figure ٣-٥: Joint strength as a function of titanium thickness [٨٠].

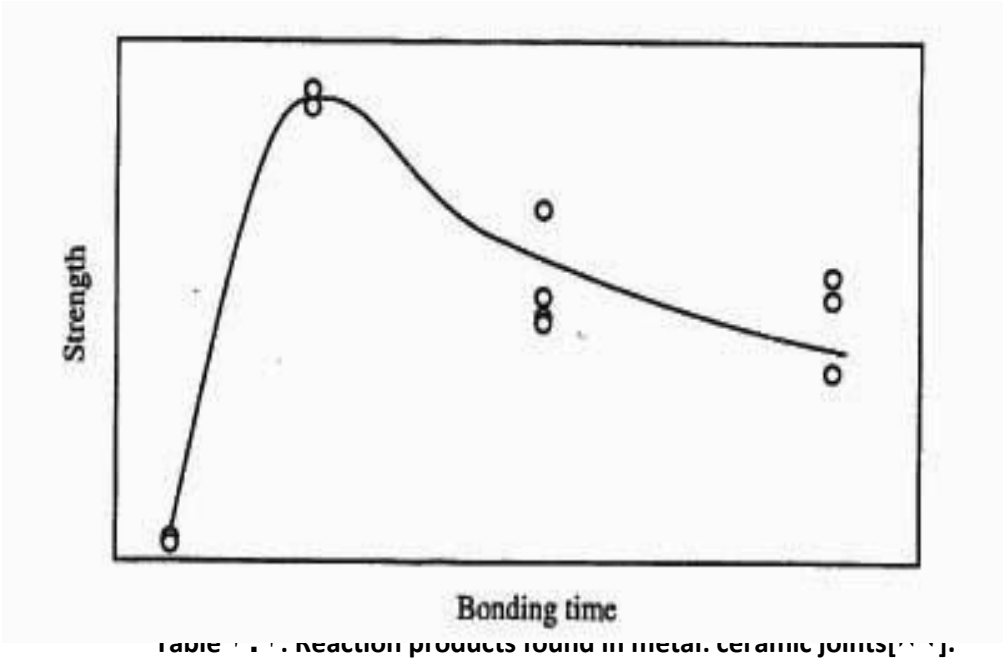

Table ٣-١: Reaction products found in metal/ceramic joints[٨١].

Ceramic	Metal	Reaction Product
Al_2O_3	Ti	TiO, $TiAl_3$
Al_2O_3	Ti	Ti_2O_3, Ti-Al-O***
Al_2O_3	Ti-Ni	Ti-Al-O
Al_2O_3*	Ti-Ni	TiO_2, TiO, Ti_2O_3, Si, SiO_y, Si-Ti-O
Al_2O_3*	Ti-Ni-Ag	TiO_2, TiO, Ti_2O_3, Si, SiO_y, Si-Ti-O
Al_2O_3*	Mo	MoO,MoO_y
Al_2O_3*	Mo	Al_2O_3, $^3MoO_3$
Al_2O_3*	Mo-Mn	MnO,MoO_3,MoO_2,MnO*Al_2O_3
Al_2O_3*	Mo-Mn	MnO,aMnO*bAl_2O_3*cSiO_2
Al_2O_3	Nb	NbO_y
Al_2O_3-CaO-MgO	Nb	NbO_y
Al_2O_3-CaO-MgO-SiO_2	Nb	NbO_y
Al_2O_3-CaO-MgO-SiO-Na_2-K_2O	Nb	NbO_y, Na, K
Al_2O_3-CaO-MgO	Ta	TaO_y
Al_2O_3-CaO-MgO-SiO_2	Ta	TaO_y
Al_2O_3-CaO-MgO-SiO-Na_2-K_2O	Ta	TaO_y,Na, K
AIN	Ta	TaN
AIN	Zr-Ni	ZrN
AIN	Ti-Ni	TiN
AIN	Hf-Ni	HfN
AIN	Nb-Ni	NbN
AIN	V-Ni	AlNi, Al_7V
AIN	Ta-Ni	AlNi, Ta_2Al, Ta_5Al_3
AIN	Cr-Ni	AlNi
AIN	Mo-Ni	AlNi
AIN	W-Ni	AlNi
SiC	Al	Al_4C_3
SiC	Mo	Mo_2C, Mo_3Si_2
SiC	Ti	Ti_5Si_3, $TiSi_2$
SiC**	Ge	Si-Ge
Si_3N_4	Ti	Ti_5Si_3, $_{TiSi}^2$
Si_3N_4	Mo	Mo^3Si, $MoSi_2$
Si_3N_4	W	W_5Si_2, WSi_2
Si_3N_4	Ta	TaN, Ta_2Si
TiC	Ti	Ti_2C, TiC_y
TiC	Mo	Mo_2C
BN	Mo	Mo_2B, MoB
BN	W	W_2B, WB, W_2B_5, WB_4
BN	Ta	TaN, Ta_2B, TaB
VC	Ti	V_2C, TiC

* contains SiO_2.

** contains free Si.

***this output of reaction product is likely happened in our investigation

۳.۳.۱ The Role of Titanium in Brazing Oxides

Titanium can dissolve ۲۹ at % of oxygen at ۱۱۲۵°C and forms a family of oxides ranging from TiO to TiO_2 as shown in Fig. ۳-۷ [۲]. Thus, in order to understand the role of titanium in the active metal brazing of oxides it is important to know which oxide will be formed as a product by reactions such as

$$3[Ti] + Al_2O_3 \rightleftharpoons 3TiO + 2[Al] \qquad (۳-۱۹)$$

in which square brackets identify solutes. If the product is assumed to be stoichiometric, the energy change ΔG_R associated with the reaction, can

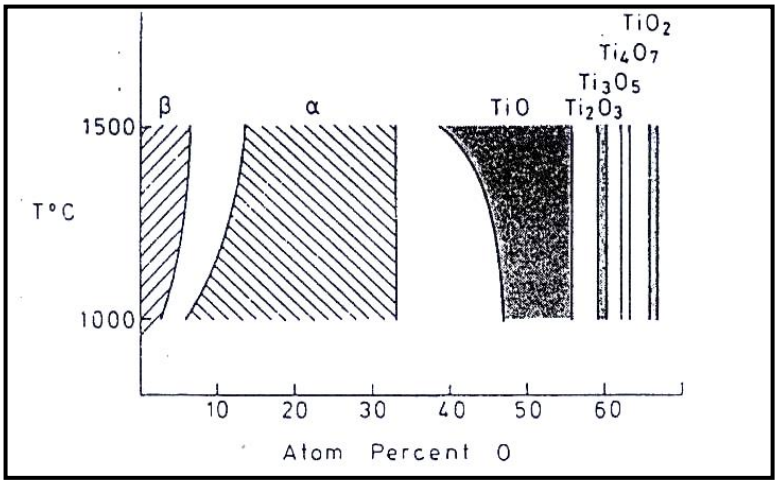

Figure ۳-۷: Ti-O Phase diagram [۲]

be related to the free energies of formation of the oxides and the metal activities by the equations

$$\Delta G_R = 3\Delta G^{\circ}_{F(TiO)} - \Delta G^{\circ}_{F(Al_2O_3)} \qquad (۳-۲۰)$$

$$= -RT \ln\left\{\frac{a(Al)^2\, a(TiO)^3}{a(Ti)^3\, a(Al_2O_3)}\right\} \qquad (۳-۲۱)$$

$$= -RT \ln \left\{ \frac{a(Al)^2}{a(Ti)^3} \right\} \qquad \textbf{(٣-٢٢)}$$

if the final simplification, the activities of the solid oxides are taken as unity. The reaction cited above will progress to the right and TiO will be formed until the activity ratio of the aluminum and titanium reaches an equilibrium value of ١.٠١ at ١١٢٥°C, or the titanium activity falls below the value (٤×١٠^{-٤} at ١١٢٥°C) needed to inhibit the formation of $Ti_٢O_٣$ by the degradation reaction[٢,٨٧,٨٨]

$$^{٣}TO \quad i\,[\text{Ti}] + \text{Ti}_٢O_٣ \qquad \textbf{(٣-٢٣)}$$

At even lower activity levels (below ٩×١٠^{-٧}) $Ti_٣O_٥$ will be formed, then $Ti_٤O_٧$ and ultimately $TiO_٢$ [٢].

Which product is formed is important because, while they are all ceramics, TiO differs from the others in being metallic, as indicated by its low electrical resistivity ($٣\times١٠^{-٤}\Omega m$ compared with ٠.٣Ωm for $TiO_٢$ and about $١٠^{١٢}\Omega m$ for $Al_٢O_٣$ [١٢]. Further, there is evidence that decreasing oxygen-to-titanium ratios can enhance wettability: the contact angles of copper in a vacuum at ١١٥٠°C decrease from ١٤٠° on $TiO_٢$ to ١١٣° on $Ti_٢O_٣$ to ٨٣° on $TiO_{١.١٤}$ and to ٧٢° on hypostoichiometric $TiO_{.٨٦}$ [٢].

Naidich and Zhuralev [٢,٨٩] who used X-ray diffraction techniques to observe the presence of TiO at the interface formed by alumina with a Cu-٢at % Ti alloy at ١١٥٠°C, while $Ti_٢O_٣$ was found at the interface formed by ٢ at % Ti in gold and nickel at ١٥٠٠°C. In practice, significantly higher titanium concentrations, in copper, have to be employed to achieve rapid and reproducible wetting, possibly because of the desirability of forming hypostoichiometric TiO[٢].

The ideal braze solvent would be one in which the activity coefficients of the reactive solutes are large. Since saturated solutions have high activities, this implies that alloying the solvent to decrease the solubility can be beneficial, as illustrated schematically in Fig ٣-٨. In this

Figure ٣-٨: Schematic illustration of the effect of varying solubility on solute activity[٢].

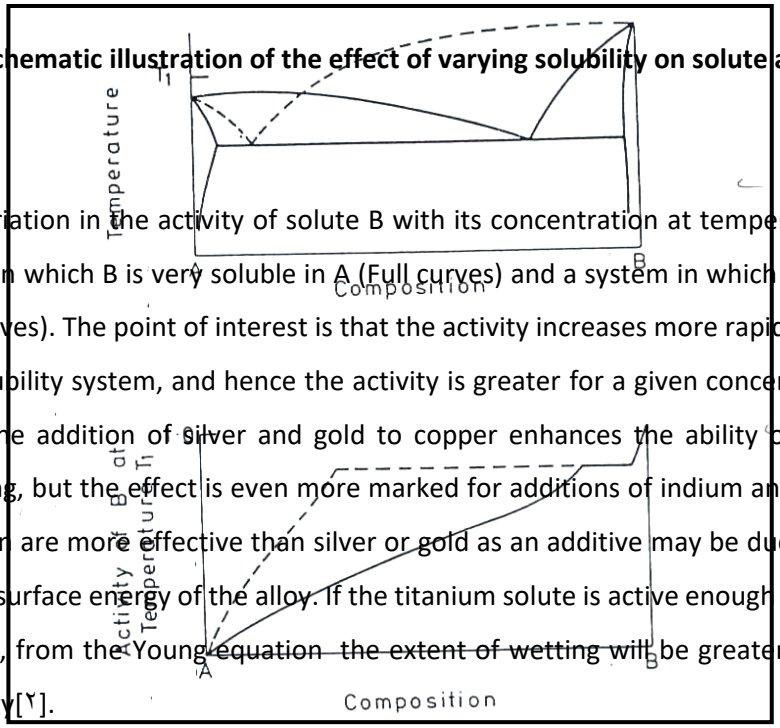

figure the variation in the activity of solute B with its concentration at temperature T_1 is illustrated for a system in which B is very soluble in A (Full curves) and a system in which B is slightly soluble in A (broken curves). The point of interest is that the activity increases more rapidly with concentration for a low-solubility system, and hence the activity is greater for a given concentration of B. Practice shows that the addition of silver and gold to copper enhances the ability of titanium solutes to induce wetting, but the effect is even more marked for additions of indium and tin. The reason why indium and tin are more effective than silver or gold as an additive may be due to their efficiency in lowering the surface energy of the alloy. If the titanium solute is active enough to cause wettable TiO to be formed, from the Young equation the extent of wetting will be greater for a liquid with low surface energy[٢].

In a set of experiments using thin- film Ti/ Ag-Cu bilayers to braze sapphire, Santella *et al.*[٩٠], noticed that if the bilayer was deficient in Ti, islands of Ti_3O_2 would form on the alumina surface, but no brazed joint was made [٩٠].

The bilayers that resulted in successful brazes formed reaction layers containing Ti_3Cu_3O with dissolved aluminum. This observation led them to claim that "Ag-Cu does not spread over the titanium oxide layer, but over Cu-Ti-O system compounds". Cu-Ti-O system compounds can be formed by the oxidation of Cu-Ti intermetallic compounds. Suenaga and coworkers proposed the following chemical reaction as are possible oxidation reaction, based on the reaction products found in their brazing experiments:

$$3Cu_4Ti + 2TiO \rightarrow Cu_3Ti_3O + Ti_2O + 9Cu \qquad \textbf{(٣-٢٤)}$$

Another common Cu-Ti-O phase is Cu_2Ti_4O , which could be formed by a similar reaction. This phase that appears is influenced by the activities of Ti and O in the joint. Ti_3Cu_3O will form if the activities of Ti and O are both low but higher Ti and O activities will cause Cu_2Ti_4O to form; these compounds are called M_2X[٣٠,٧٩,٩١].

٣.٣.٢ Titanium Scavenging From the Active Filler Metal

Poor hermeticity was observed for Al_2O_3 / Al_2O_3 braze joint using a Fe-٢٩Ni-١٧Co alloy space and Ag-Cu-Ti active metal[٩٢].

P.T Vianco and several other coworker have published a series of papers [٩٢-٩٣] studying the scavenging mechanism of active element. Titanium was scavenging from the filler metal by formation of a (Fe, Ni, Co)-Ti "lacework" phase.

They have claimed that process parameter did not circumvents the loss of Ti to (Fe, Ni, Co)-Ti phase development when brazing to bare kovar (Fe-٢٩Ni-١٧Co) alloy but titanium scavenged from the filler metal resulting from dissolution of the kovar™ interlayer in the braze joint.

Vianco *et al.*, [٩٢] used three approach to minimize and eliminate of Ti scavenging from the filler metal to braze Al_2O_3 / kovar/ Al_2O_3. First approach: A molybdenum barriers layers sputtered on the kovar surface, did successful prevent Ti scavenging, resulting in continuos Ti_xO_y layer formation at the filler metal / Al_2O_3 interface an hermetic joint. The brazing temperature ٨٥٠°C for ٥ min.

Second approach: A ١٠٠٪ Mo interlayer showed that the values of thickness Ti_xO_y were nearly twice those which resulted from use of the Mo-coated kovar. The third approach: Using Zr as the active element in Ag-Cu-Zr filler metal and they was found to be essentially immune to the scavenging phenomenon, resulting in strong hermetic joints at high processing temperatures.

In a similar study Vianco *et al.,* [٩٣] used a Mo barrier coating on Fe-٢٩Ni-١٧Co space by deposited with thicknesses of ١٠٠, ٢٥٠, ١٠٠٠, ٢٥٠٠, ٥٠٠٠ Å to prevent formation "lacework" phase, they should the thickness ٢٥٠ Å. Mo coated spaces have excellent strength and produced hermetic joints at the temperature ٨٥٠°C for ٣ or ٥ min. The fracture surface in all case was located at the interface between the alumina and the filler metal excepts specimens mad with the ٥٠٠ Å Mo coated.

The authors have successfully another technique to prevent Ti scavenging from filler metal. They used ١٠٠٪ Fe, ١٠٠٪ Ni, ١٠٠٪ Co spacers between Al_2O_3 / Al_2O_3 joint and they found that:(١) Fe spacer caused the development of Fe_x Ti_y phases at the interface with Ag-Cu-Ti filler metal and formation of a significant Ti $_x$ O_y layer occurred at the Ag-Cu-Ti / Al_2O_3 interface resulting in ١٠٠٪ of the braze joint being hermetic.

(٢) Co spacer resulted in the development of a lace-work phase having Co_3Ti and potentially metastable Co_x Ti_y compositions A thin intermittent Ti_xO_y reaction layer was observed at the AgCuTi/Al_2O_3 interface resulting in only ٧٥٪ the button being hermetic.

(٣). Ni spacer caused an extensive Ni_3Ti phase to form at the AgCuTi/Ni interface as well as discrete Ni_3Ti phase particles to develop in the filler metal. Cu-Ni solid solution phase was also observed at the Ni- spacer interface complete scavenging of Ti resulted in the absence of a Ti_xO_y layer at the Ag-Cu-Ti / Al_2O_3 interface and zero percent of the braze joints were hermetic[٩٣].

٣.٣.٣ Influence of Substrate Materials on Reaction Products

When alumina is instead brazed to a metallic substrate, the elements in the base metal diffuse to the filler metal **/** ceramic interface and influence the reaction product that form. When alumina is brazed to titanium-based alloys, titanium from the base metal supplements the titanium already present in the filler metal, increasing the activity of the titanium in solution. Increased Ti activity can change the reaction products that form, most notably Ti_4Cu_2O rather than Cu_3Ti_2O. Very high Ti activity can suppress the formation of Ti-Cu-O compounds to instead form Ti_2Cu [٩٥]. Also, since a large amount of Ti present will cause more Al_2O_3 to be reduced, the result is a thicker reaction layer, and the formation of titanium oxides rich in Ti, such as Ti_2O rather than TiO [٩٥-٩٦].

Using commercially pure copper as a substrate doesn't significantly change the reaction products that formed because Cu is already presented in the filler metal, the morphology of the braze is different, most noticeably in the increase segregation between the Ag and Cu in the braze metal near the reaction layer, the reaction layer of this type of joint was reported to be about ٠.١ μm thinner than that for an alumina-alumina braze [٧٩].

When stainless steel was used as the substrate material, the reaction products changed due to the addition of iron, nickel, and chromium to the system. The nickel and chromium have been reported to diffuse evenly through the braze alloy into the reaction layers without forming detectable amounts of reaction products. Iron , on the other hand, will react with TiO to form Fe_2Ti_4O. Lee and coworker[٧٩] believe that this compound and the Cu-Ti-O compound are found together as (Fe, Cu)$_2Ti_4O$. Evidence of a Ti-Fe intermetallic compound was also found, and the additional reaction products cause the reaction layer to be slightly thicker than that presented in an alumina-to-alumina braze [٧٩].

Examination of phase diagrams can help to predict how the substrate material will influence the chemical reactions that occur during the brazing process. Fig.٣-٩ compares the Fe-Cu and Ni-Cu phase diagrams [٩٧-٩٨]. It is evident that Ni and Cu form a solid solution but Fe and Cu are immiscible, therefore Ni-and Fe based alloy will interact with Ag-Cu filler metals differently.

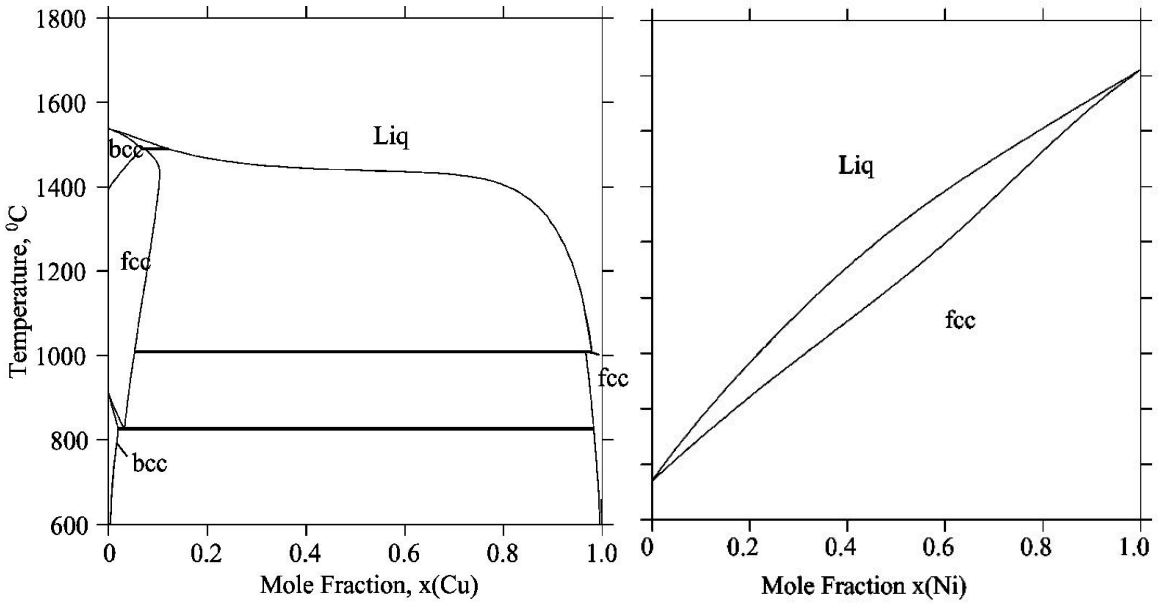

Figure ٣-٩: Binary phase diagrams : (L) Fe-Cu (R) Ni-Cu [٩٧-٩٨].

٣.٤ Residual Stresses from Cooling

the ultimate goal of any joining process is to produce a reliable joint. Hence, any factors that control or effect the joint strength must be studied in detail and efforts directed to the manipulation of appropriate variables. The ability to accommodate stresses due to thermal expansion mismatch between components is the primary mechanical problem facining ceramic metal joint.

Almost all processes for ceramic-metal joining require raising both the components to a temperature considerably high than room temperature. This is true for brazing and plasma spraying as well as for diffusion bonding. At the joining temperature, both components are in mechanical equilibrium. As the components cool from the joining temperature, the high thermal expansion material shrinks more than the low thermal expansion material. At a room temperature, the low expansion material experiences a predominantly compressive stress, while the high expansion material is in tension Fig. ٣-١٠[٤] .

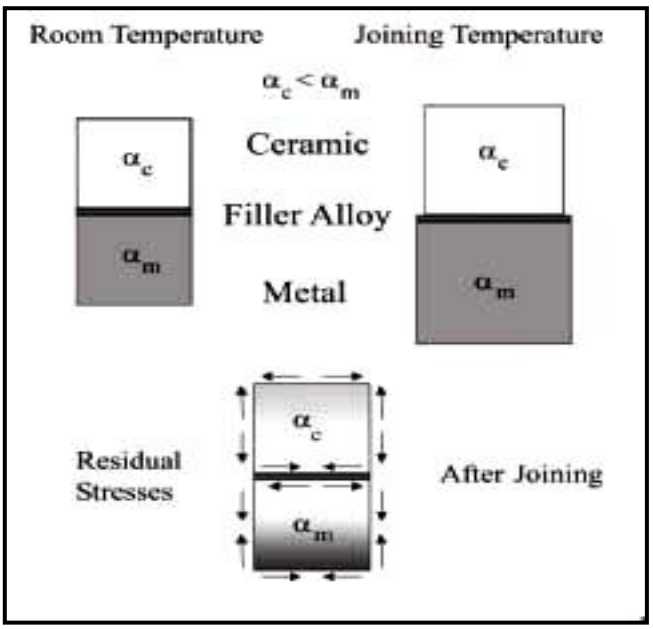

Figure ٣-١٠: Schematics of residual stresses developed during joining process [٤].

From the standpoint of fracture mechanics, this is fortunate, as low thermal expansion materials tend to be brittle Table ٣.٢.

Table ٣.٢: Thermal expansion and elastic modulus data for several material[٧]

Materials	C.T.E. ($x١٠^{-٦}$ $°C^{-١}$)	Young's Modulus (GPa)
Fe	١٢.١(١٠-٢٠٠°C)	٢١٠
Cu	١٧.٢(٠-٢٠٠°C)	١١٥
Invar	٢.٠(٣٠-١٠٠°C)	١٤٧
Kovar	٦(٣٠-٥٠٠°C)	١٤٧
SUS ٣٠٤	١٧.٨(٠-٣٠٠°C)	٢١٠
$Al_٢O_٣$	٨ (٢٥-)	٣٦٠
$ZrO_٢$	١٠.٠(٢٥-)	١٣١
MgO	١٣.٣(٢٥-)	٨٥
$Si_٣N_٤$	٣.٧(٤٠-٨٠٠°C)	٢٩٤
Inconel ٦٠٠	٦.٧(٢٥-)	٢١٧
Ti	٩.٧(٢٥- ٦٠٠°C)	١١٧
W	٤.٦(٢٥-٥٠٠°C)	٣٥٠
Mo	٥.٧(٢٥-٥٠٠°C)	٣٢٩

The measured strength of any joint reflects the true bond strength minus the residual stress. Hence, strength data on ceramic/ metal joints is obscured by the effect of residual stress which is a very sensitive function of both component properties and joint geometry. It is intuitive that materials with a great disparity in thermal expansion will be more difficult to join than materials that are identical. As this mismatch increases, the likelihood of failure increases accordingly [٩٩]. High strength materials exacerbate the effect of thermal expansion mismatch because the mismatch energy is stored elastically, concentrating the residual stress along the interface of the joint.

Processing variables such as joining temperature and cooling rates are generally determined by the method used to join the components. Rapid cooling rates, associated with processes that use localized heat sources, can increase residual stress due to the presence of thermal gradients within components and the inherently greater deformation resistance of materials at high strain rates. Generally, residual stress scales with the deviation from bonding temperature, making processes using the lowest possible bonding desirable.

Another important consideration is the geometry of the components that form the joint. For cylindrical butt joints measured with a strain gauge, the stresses were found to increase with increasing bonded area, making it difficult to form joints of large cross-sectional area [٨]. In addition, rectangular components with stress-risers created by their sharp corners were found to have higher stresses than similar cylindrical joints Fig. ٣-١١.

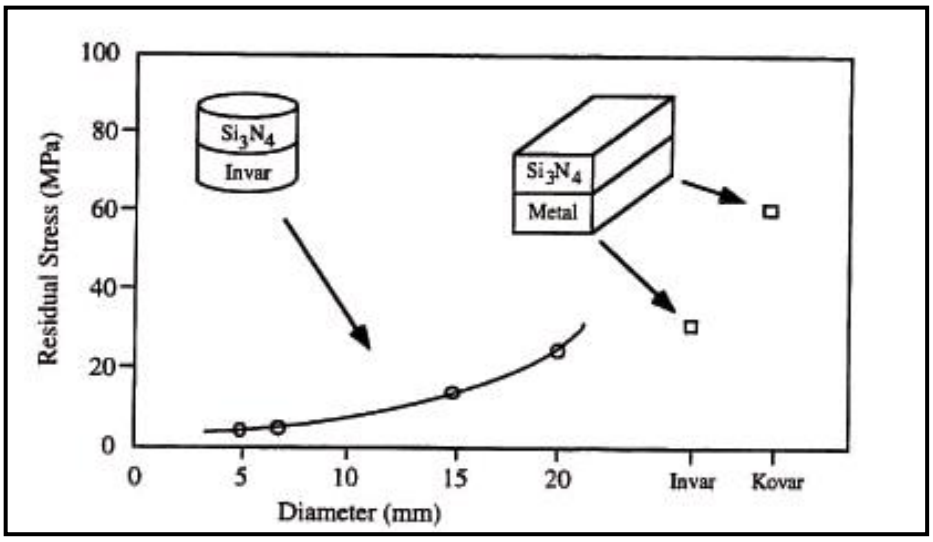

Figure ٣-١١: Residual stress as a function of bonded area and geometry [٨].

The use of a low flow stress material such as aluminum is often used to dissipate residual stress plastically [٥]. As the joint begins to cool, the thermal strain energy that begins to develop is minimized by the deformation of the aluminum. This method is most effective when chemical reactions do not occur and the cooling rate is slow enough to allow for some degree of mechanical equilibration. This type of process can not be used for high temperature applications due to the effects of creep.

Thermal expansion mismatch can also be controlled through the use of functionally gradient materials. By using interlayers with thermal expansions that gradually increment from the low expansion material to the high expansion material, each layer absorbs only a small portion of the total mismatch [٨-٩]. The residual stress can be minimized by increasing the number and thickness of the interlayers.

For high strength materials with a large thermal expansion, cracking may occur as the joint cools down from the joining temperature. Residual stress, concentrated at the interface is a driving

force for crack propagation in dissimilar material joints. In practice , porosity or flaws at the interface are frequently the site of failure initiation [٧].

٣.٤.١ Theoretical Stresses Present at the Jointed Interface

The residual thermal stresses and strains presented in the joint shown in Fig. ٣-٩ can be solved by using Hook's law ($\varepsilon = \sigma/E$) and the thermal strain relationship ($\varepsilon = \alpha \Delta T$). For the simple case of two purely elastic materials perfectly bonded over a unit area at high temperature, the magnitude of the residual stresses is presented at the interface in the base metal after cooling to room temperature T, in the plane stress condition, is derived to be[٧]:

$$\sigma = \frac{E_M E_C}{E_M + E_C}(T_{bond} - T)(\alpha_M - \alpha_C) \qquad (٣-٢٥)$$

E is Young's modulus and α is the linear coefficient of thermal expansion. Equilibrium requires that the forces (stresses) balance. The stress in the ceramic is equal but opposite ($\alpha_C - \alpha_M$).

Residual stresses can also be expressed in terms of strain energy, the energy that is stored in the strained material. The strain energy U, is expressed by integrating the stress over the displaced area[٩]:

$$U = \int \sigma \, d\varepsilon \qquad (٣-٢٦)$$

For the planar butt joint in Fig. ٣-١٠ the strain energy at the interface in the metal component at room temperature T is

$$U = 1/2 \frac{E_M E_C}{E_M + E_C}(T_{bond} - T)^2(\alpha_M - \alpha_C)^2 \qquad (٣-٢٧)$$

since the CTE term is squared, the same strain energy is presented in the ceramic as in the metal.

٣.٤.٢ Characterization of Residual Stresses in Complex Systems

The stress state in the joint becomes significantly more complex when the ductile filler metals is included in the analysis and all the three dimensions of stress are considered. There are experimental ways to measure residual stress; these methods are very time consuming and not used as prevalently as computational methods, but they will be mentioned for completeteness. Self compensating type strain gauges can be pasted to the surface of brazed joint, and when the joint is cut (relieving residual stresses) the difference in strain recorded by the gauge can be translated into residual stress. X-ray diffraction of stressed material can measure changes in the crystal lattice parameter, which can be used to calculate residual strain and stress. These techniques were used in studies published by Suganuma and Okamoto , Iance *et al.,* respectively [٨,١٠١] , but they were unable to find a unique trend from their variables

Modeling work has also been done on metal-to-ceramic brazed joints. Kweon and Xhoi[١٠٢] successfully predicted the location of residual stress induced cracking in an alumina-carbon steel cylindrical butt joint from the location and direction of the maximum principal stresses. Fig. ٣-١٢ shows a sketch of where the cracks were predicted to occur and all the three categories of cracks were observed in the actual brazed joint, and the stresses calculated through the XRD method were in qualitative agreement with those calculated by model.

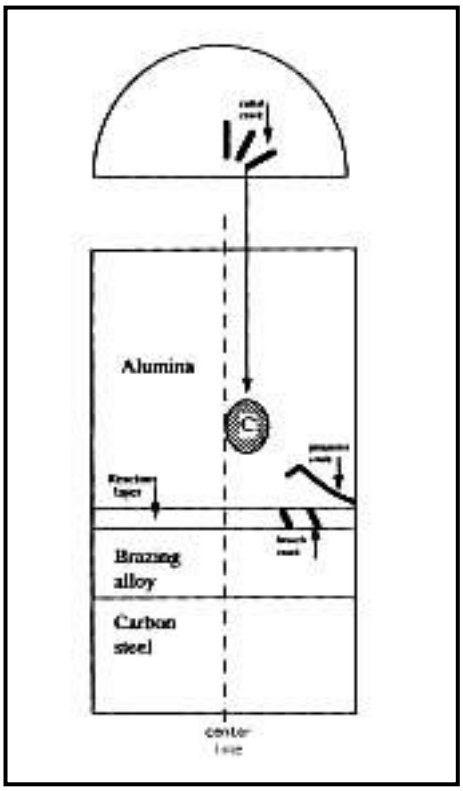

Figure ٣-١٢: Predicted cracks in alumina-carbon steel brazed joint [١٠٢]

٣.٤.٣ Finite Element Analysis Applied to Ceramic-Metal Joining

Numerical methods such as FEM are often used to solve for the stress state in dissimilar materials joints. A common goal of many of the finite element models is to predict where residual–stress induced cracking will occur and how the joints will fail under external loading.

Finite element methods have also been used to theoretically optimize interlayers bonding metallic and ceramic substrates optimized the properties of functionally graded interlayer to reduce the predicted maximum tensile stress in the ceramic .In a comprehensive study of cylindrical (metal around ceramic) lap joint, Selverian and coworkers examined how interlayers influenced the residual stresses of Incoloy ٩٠٩-$Si_٣N_٤$ and Inconel ٧١٨-$Si_٣N_٤$ joint [١٠٣]. They found that a high expansion, low flow stress interlayer (nickel) was more effective in reducing the residual stress in the ceramic than a low expansion, high flow stress interlayer (molybdenum) or a low expansion, low flow stress interlayer (hypothetical material). Their model showed that when a low expansion interlayer was used, the expansion mismatch between the interlayer and structure metal resulted in additional stresses being transferred to the ceramic component. Their calculations also showed that the properties of the base metal contributed significantly to the radial stresses in the joint but only slightly to the axial stresses.

Suganuma *et al.,* [١٠٤] used diffusion bonding to produce a series of joints, one of these series describes a model based on the finite element method which it is possible to determine the maximum residual stress in the joint both with and without the interlayer material. Simple mesh generation used of the joint configuration consists of two cylindrical specimens joined end to end

with a variable interlayer thickness. The two base materials in this study were alumina and a ferritic steel. Some of the important assumption in this model included (i) all physical constants were assumed to be independent of temperature and assumed constant. (ii) All materials were assumed to behave elastically.

Graphics are often used as a type of simulations. An example of this illustrated by the elastic finite element analysis of the maximum principle residual stress at room temperature for a silicon nitride / steel joint formed at ٨٠٠°C [١٠٥]. The stresses are dependent upon the location within the joint and tend to peak along the interface of the joint, near the free surface Fig.٣-١٣.

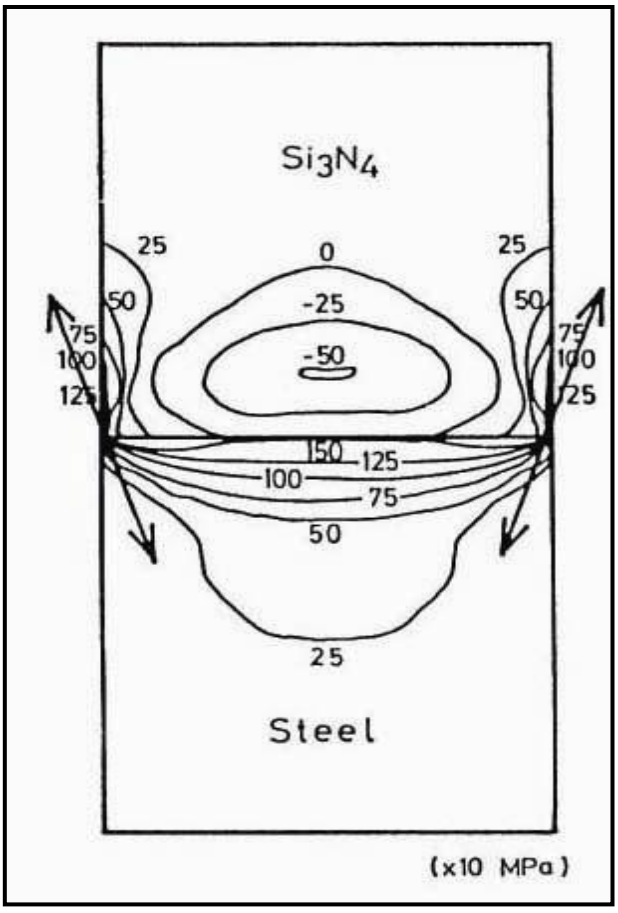

Figure ٣-١٣: Contour map of internal stress following cool down from ٩٧٥°C to room temperature.. Arrows represent maximum tensile stress in silicon – nitride [١٠٥].

Martinelli *et al*.[١٠٦], studies the distribution of residual stresses in SiC-Mo joints along a line perpendicular to the SiC-Mo interfaces. This behavior was studied by FEM analysis. Three – dimension thermal elasto-plastic model was generated to study those joints. A preliminary analysis was performed considering both materials as ideally linear-elastic components. Subsequently, a model where only the ceramic was considered to be linear-elastic throughout the thermal loading was constructed. In this case, the metallic component was modeled considering an elastic perfect-plastic behavior, the Von Mises yield criterion, and the associative Prandtl- Reuss flow rule. Because of the typically high joining temperatures, the variation of the mechanical properties of the material with temperature must by considered, especially young moduli, linear coefficients of thermal expansion, as well as yield strength and tangential modulus of the metal. Poisson's ratio could be assumed to be constant. The symmetry of the joined couple with respect to geometry, mechanical properties, and loading may allow significant simplification of the model. Only one quadrant of rectangular joints, such as the illustrated in Fig.٣-١٤a can be modeled. A sequence of finite mashes was then built. Firstly , a uniform mesh composed of trilinear hexagonal elements was considered. Subsequently, to improve the accuracy of the analysis near the interface (region of stress concentration), a triquadratic mesh was considered Fig. ٣-١٤b. In addition , sample cooling was assumed to occur free from mechanical loads. The temperature distribution inside the diffusion couple was assumed to be uniform, to avoid the need to solve a heat-transfer equation during the iterative process[١٠٦].

FEM analysis may also provide a complete map of all stress components, including shear stresses, which are particularly hard to obtain experimentally. An example of principal stresses and Von Mises stress maps obtained from Fe-Ni-Co/Al_2O_3 and Cu-Mo(elastic) brazed joint are shown in Fig٣-١٥(a,b) respectively [١٠٧].

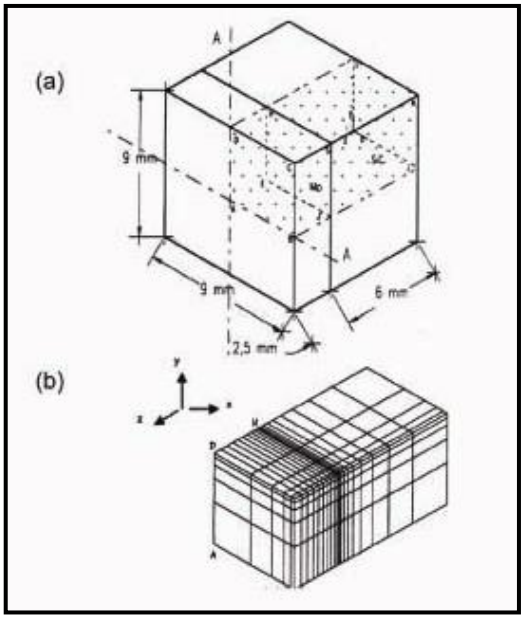

Figure ٣-١٤: (a) Overall sample and modeled quadrant and (b) modeled mesh[١٠٧].

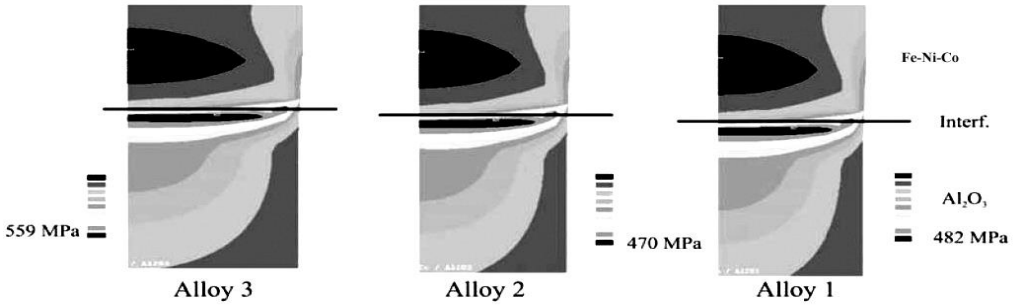

a

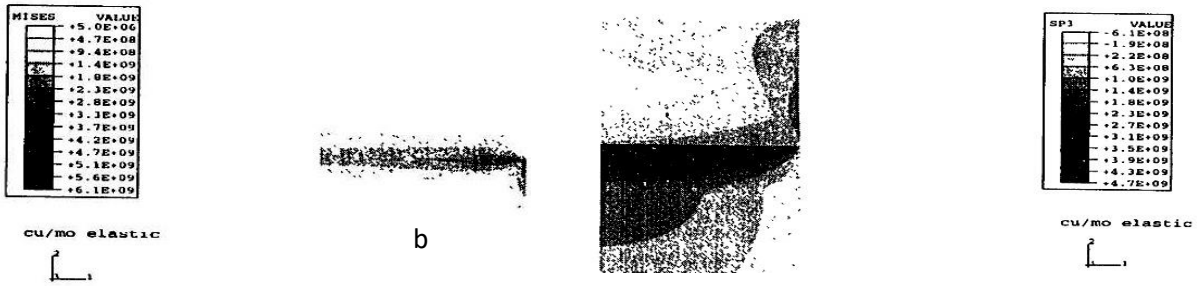

b

Figure ٣-١٥: Distribution of residual stresses(a) principle stress S_1

for Fe-Ni-Co/Al_2O_3 joint[١٠٧](b) principle stress S_1 and Von Mises stress for Cu-Mo joint[٤]

٣.٥ Shear Strength of Metal-to-Ceramic Brazed Joints

Strength measurements of ceramic-to-metal are important to provide information on mechanical integrity of the joints. In covenvetional testing of metal-to-metal joints, the stress to fracture is used to characterize the bond strength of the interface. However, the failure stress of ceramic-to-metal joints is strongly influenced by residual stresses induced in the joint as well as the quality of the interface [٢].

The mechanical testing of ceramic-to-metal joints has not been standardized[٢,٤].Fig ٣-١٦. illustrates the configurations of three-point bending, four point bending, and shear test that have been frequently used to measure ceramic-to-metal joint strength .Since different fracture strength and patterns can be observed even with the same material combinations depending on the joint geometry and testing methods, the testing should be done as closely as possible to the real joint design and service conditions [٢].

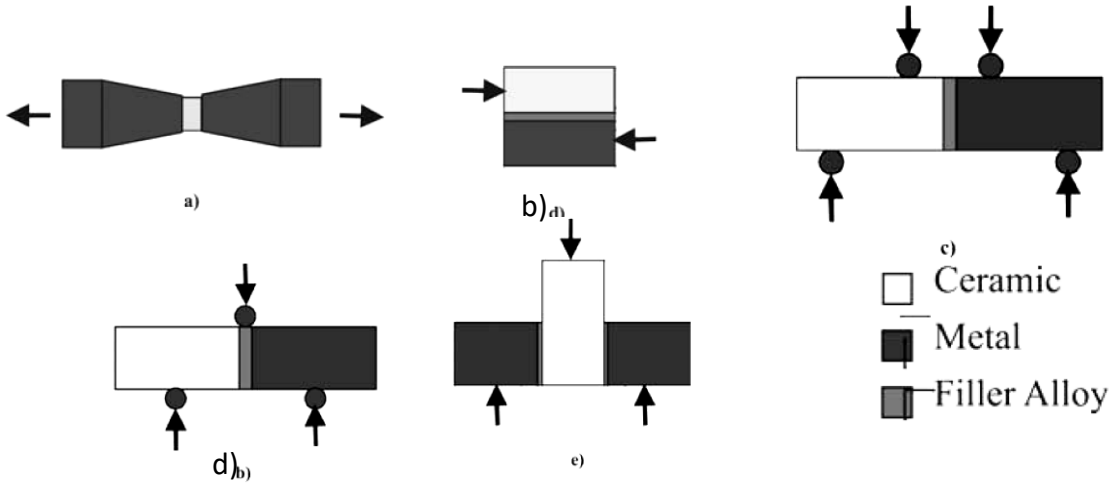

Figure ٣-١٦: Schematic illustrations of five common type of tests for ceramic-metal joints;(a)tensile (b) plain shear (c) ٤-point bending (d) ٣-point bending (e)shear on ring/ cylinder[٤].

٣.٥.١ Influence of Processing Conditions on Joint Strength

There are many conditions which can affect the reaction products present in the brazed joint. The chemical activity of the elements, reactions that will occur at the interface, and thickness of the reaction layers are all dependent on both the brazing temperature and time. Additionally, the cooling rate affects the strain rate in the filler metal, which can influence the residual stresses present in the joint.

A study on the strength of Al_2O_3 – titanium joints brazed with Ag-Cu-Ti filler metal determined the optimal brazing parameters for the system [٩٦]. This system is unique because the base metal is the same as the reactive element in the filler metal. The parameters were optimized for both shear strength and corrosion resistance. Temperatures were between ٨٥٠-٩٥٠°C for

holding times between ٥-٤٠ minutes. For the higher brazing temperatures, though, joint strength was optimized for a holding time of ٢٠ minutes.

Micrographs of the fracture surface show how the fracture path varied with the processing parameters (microstructure). The strongest joints exhibited mode I crack initiation in the location of highest tensile stress in the ceramic, but mode II propagation in the ceramic near the interface. The majority of the joints had the cracks initiate in the ceramic near the interface, but the crack path moved into and propagated through the filler metal. The weakest joints had cracks propagate exclusively though the interface between the alumina and filler metal.

Lee brazed Si_3N_4 to Inconel ٧١٨ using Ag-Cu-Ti filler metal, at temperatures ranged between ٧٩٠-٩٠٠°C for holding times between ٧-٥٠ minutes and tested the strength of the joint in shear, tension and bending [١٠٨]. He found that the optimal brazing temperatures for joint strength was ٧٩٠°C for ٢٠ minutes for his system; he also noted that brazing temperature was more important than brazing time for controlling the reaction products presented in the joint. At high temperatures, the titanium in the filler metal tended to diffuse into the base metal rather than toward the ceramic surface, which compromised the strength of the joint. He showed that the strongest joints, the crack initiated at the edge of the interface and propagated through the ceramic perpendicular to the interface.

٣.٥.٢ Influence of Joint materials on Joint Strength

The strongest joints made by Lee between Si_3N_4 and Inconel ٧١٨ had a shear strength approximately half that of joints made between Si_3N_4 and Inconel ٦٠٠ that they had previously made in their laboratory. Inconels ٦٠٠ and ٧١٨ have nearly an identical thermal expansion behavior, but difference chemical composition and yield stresses [١٠٨]. Lee attributed the difference in strengths in the joints to the different morphologies and reaction products observed in the joints, but it is possible that the large difference in yield stress between the metals (٥٥٠-٦٨٠ MPa for cold-drawn Inconel ٦٠٠ at room temperature compared to ١١٠٠ MPa for precipitation hardened Inconel ٧١٨) caused the stress state in the bonded ceramic to differ, resulting in different joint strengths.

Lee *et al*. also studied the strength of joints made between alumina and Inconel ٦٠٠ using Ag-Cu-Ti filler metal and ductile interlayers [١٠٩] . The interlayers influenced the type and severity of cracks observed in the alumina component of the brazed joint. Joints with no cracks were successfully made using Cu and Nb interlayers with optimized joining temperatures, durations, and

cooling times. One interesting result, with respect to cooling time, was the presence of an optimal cooling time- rapid cooling increased residual stresses while extra slow cooling resulted in overreaction and degradation of the interface.

Selerverian and Kang extended their finite element study concentric lap joints between Si_3N_4 and Incoloy ٩٠٩/ Inconel ٧١٨ to include a study on joint shear strength under torsional loading [١١٠]. The joints tested at room temperature failed in the ceramic without exception. The shear strength of the joints made with Incoloy ٩٠٩(with a Ni interlayer) were roughly twice as strong as the joints made with Inconel ٧١٨ (with a Mo interlayer). The difference in strength can be attributed both to the higher CTE of Inconel and lower CTE and flow stress of Mo.

The joints tested at elevated temperature (٦٥٠°C) failed differently. In all cases, the joints made with Incoloy (with Ni interlayer) “slipped) without fracturing the ceramic. Auger analysis of the fracture surface showed a complex fracture path through the ceramic, reaction layer, and filler metal. The same failure mode was observed in the Inconel joint with Mo interlayer tested at ٩٥٠°C. Selvarian and Kang attributed the “slipping” at high temperatures to a decrease in the shrink–fit at the metal component around the ceramic component combined with a decrease in the yield stress of the filler metal at high temperature.

٣.٥.٣ Influence of Microstructure and Composition of the Interface on Joint Strength.

The presence of intermetallics (usually brittle) along with the thickness and morphology of reaction layers can drastically enhance or dwindle the strength of the joint. The presence of organic material or impurity particles either on the surfaces to be joined or in the filler alloy is deleterious to the interfacial microstructure. Joining defects are created. These areas of joining discontinuities increase local stresses and promote crack nucleation and growth as shown in Fig. ٣-١٧ [٥]. In particular ceramics are quite susceptible to the presence of microcracks and area of high local stresses. Upon cooling, the ceramic is often submitted to tensile stresses capable of growing existent cracks and nucleating new one.

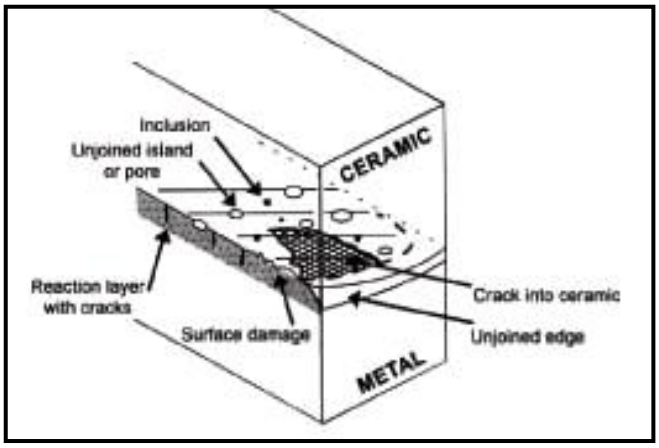

Figure ٣-١٧: Schematic representation of possible defects present in joint components [٥]

٣.٦ Fracture and Strength of Ceramic-to-Metal Joint

٣.٦.١ Fracture at Ceramic-Metal Interfaces

Interfacial Fracture Energy in Ceramic-Metal Joints

Fracture energy of the interface between two dissimilar materials exerts a critical influence on many technically important problems, particularly, the mechanical properties of composites[٦]and decohesion of films[١١١]and coatings, as well as the strength of bonds. In most oxide-metal interfaces, the fracture energy of the interface, Γ_i, exhibits relatively large values as compared to the thermodynamic work of adhesion W_{ad}[١١١],although the W_{ad} is still expected to have major influence in fracture of the interface.

The major non-thermodynamic contributions to the increase of interface fracture energy in planar interfaces are[١١٢]:

١-Rough interface

٢-Plasticity with resulting energy dissipation

٣-Phase angle,ψ

$$\psi = tan^{-1}(K_{II}/K_I) \qquad (٣\text{-}٢٨)$$

K_I where K_{II} are the mode I and he mode II crack intensity factors, respectively.

The contribution from the rough interface is based on toughening or shielding by segregated elements or roughness created intentionally or by reactive phase formation[٦].Plastic energy due to crack tip blunting or ductile void growth at the interface due to plasticity of one of the base materials increases Γ_i.This can become a major influence particularly when there is not thick interphase or reaction product at the interface [١١١].The phase angle ψ represents the relative shear to opening at the crack tip and is strongly influenced by the choice of test method. Γ_i can vary appreciably depending on ψ as shown in Fig ٣-١٨.

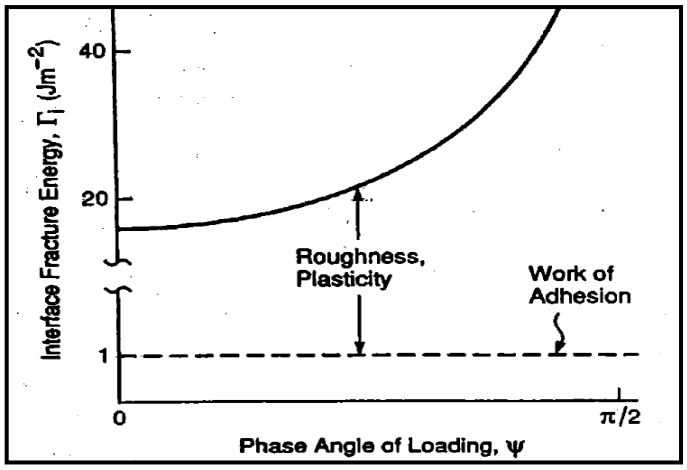

Figure ٣-١٨: Schematic diagram indicating the various fracture mechanisms that occur at metal-ceramic interfaces[٦]

٣.٦.١.١ Effect of Interface Structures

In measuring interfacial fracture energy, quantifying contributions to the fracture energy from different sources is nearly impossible. Instead, analyzing fracture mechanisms can assist in determining the dominant contributions to the interfacial fracture energy in ceramic- to- metal joints[٦].

Evans and Daglerish investigated fracture mechanisms in term of the interfacial structure and microstructure [١١١].Their test specimen and method to measure Γ_i have been carefully designed to minimize the effect of residual stresses and to prevent the crack from deviating from the interface. A thin metal interlayer was sandwiched between two thick ceramics with $\psi=\pi/٤$ which encourages interfacial cracking. Fig.٣-١٩ shows the framework which they developed to discuss the effect of interfacial structure on the fracture mechanism[١١١].Although the model systems used in their work were limited to $Al_٢O_٣$-Metal systems, the general trends are applicable to non-materials-specific systems.

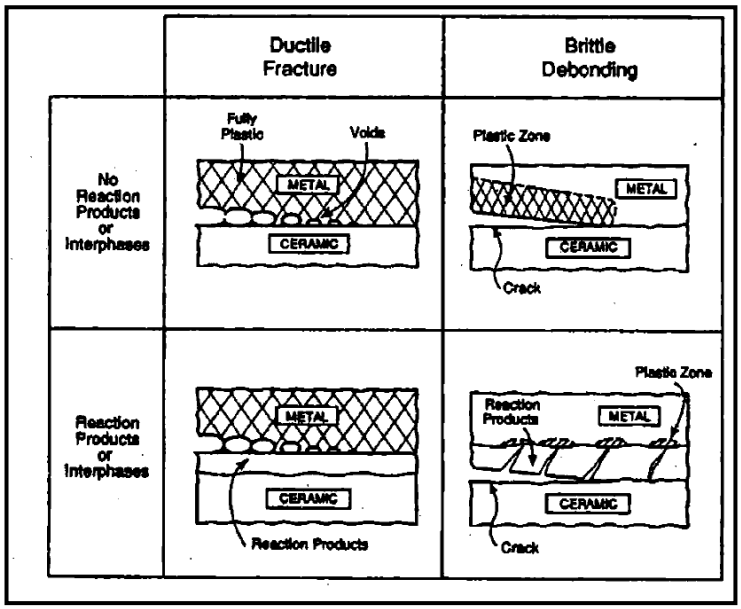

Figure ٣-١٩: Schematic diagram indicating the various fracture mechanisms that occur at metal-ceramic interface[١١١].

The ductile fracture mechanism can be described by nucleation, growth, and coalescence of voids occurring by plastic flow in the metal adjacent to the interface[١١١]. These characteristics are found on the fracture surfaces as shown in Fig.٣-٢٠ which indicates a network of metal attached to the surface caused by void coalescence. With the thin metal interlayer Γ_i scales approximately as $\sigma_o \varepsilon_o h$ where h is the thickness of the metal layer, σ_o is a uniaxial yield stress and ε_o is yield strain of the metal. This provides a framework for interpreting results of ductile fractures in the interlayer adjacent to the ceramic.

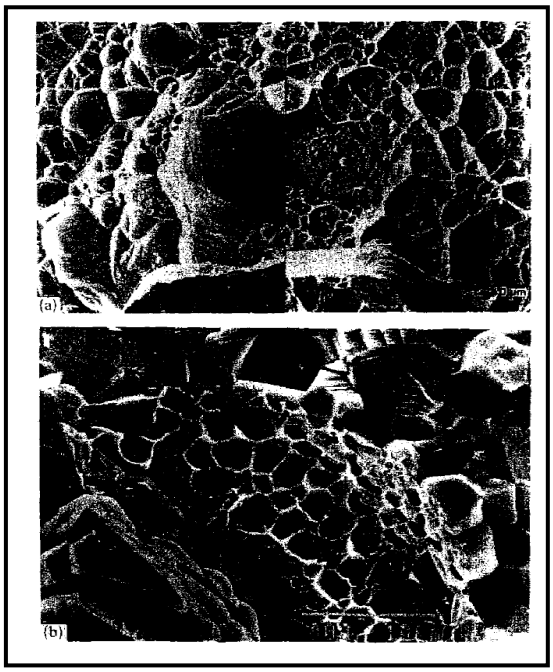

Figure ٣-٢٠ : Fracture surfaces formed when the interface fails by a ductile mechanism, obtained for the Al/Al٢O٣ system: (a)matching fracture surfaces at low magnification,(b) a high resolution view of the Al٢O٣ side of the fracture indicating a network of Al attached to this surface caused by void coalescence [١١١].

Fracture energy in the two brittle debonding examples indicated in Fig.٣-١٩ scales differently .If the interface has no reaction products, Γ_i scales with $\sigma .\varepsilon .h$,but it is considerably smaller than that obtained when the interface fails by ductile fracture as there is no reaction product. On the other hand, Γ_i is often closely related to the fracture energy of the interfacial material itself for reaction layer dominated interfaces; amorphous interfaces lead to Γ_i in range of ٥-١٠ $J.m^{-٢}$,crystalline oxide ١٠-٢٠ $J.m^{-٢}$,and intermetallics ٢٠-٤٠ $J.m^{-٢}$.This ranking generally applies despite considerable complexity in the local details of the fracture.

Microstructures of fractured interfaces are different for the two types of brittle fractures. With no reaction bonding at the interface, there is no metal attached to the ceramic, which indicates that the crack extended by brittle rapture on the interfacial plane. When there is reaction layer ,a periodic array of microcracks are found in the reaction layer, the formation and coalescence of which produce fracture[١١٣-١١٤].This mechanism is most effective when the reaction layer is thick and residual tensile stresses exist due to higher CTE of the reaction layer as compared with the ceramic. In this case, there appears to be no contribution of plastic energy to Γ_i.

٣.٦.١.٢ Effect of Residual Stresses

Evans[١١٢]schematically described an interfacial fracture mechanism between brittle and ductile materials in terms of relative fracture energy Γ_i / Γ_s and ψ as shown in Fig.٣-٢١,where S is the brittle member (ceramic) and F is the ductile member (metal).When ψ is positive (in accordance with sign convention in Fig..٣-٢١),depending on its magnitude, kinking of a crack out of the interface into the ceramic occurs, even when Γ_i is smaller than Γ_s. However when ψ is negative, the large fracture energy of the metal compared to Γ_i prohibits propagation of the crack away from the interface. One of the two possibilities can occur, depending on the yield stress of metal. For a metal with low yield stress, the failure often occurs by ductile failure as noted previously.Alternativly, the stress field of the interfacial cracks interacts with preexisting flaws in the ceramic which causes cracks to grow towards the interface, resulting in the serrated fracture with "chips" of brittle material attached to the fracture surface.

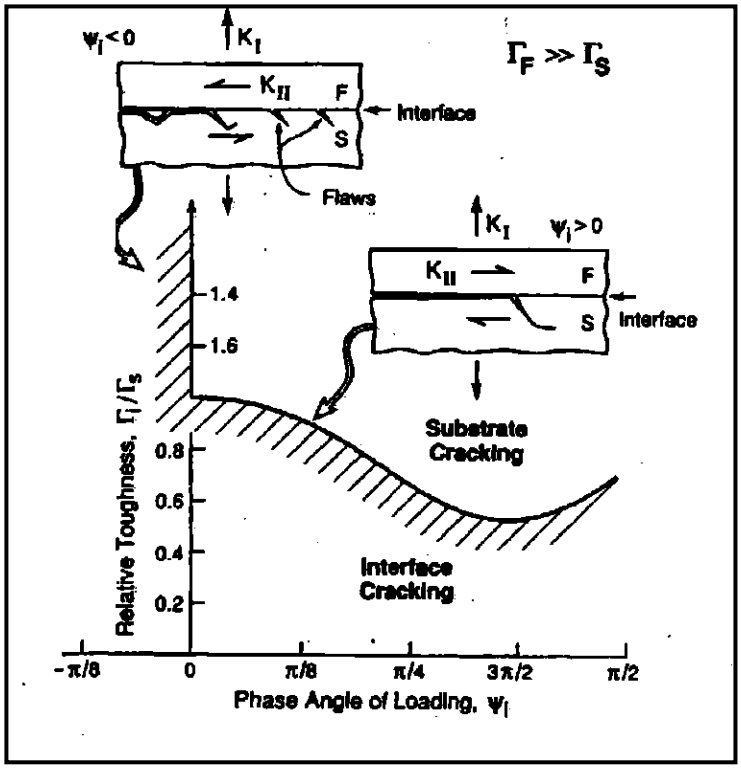

Figure ٣-٢١: Crack path diagram in interface cracks: A metal/ ceramic interface indicating the expected behavior at negative phase angle[١١٢]

Cao *et al*., investigated the effect of residual stresses on the interfacial fracture by calculating the stress intensity factor at the crack tip in the joint of two dissimilar ceramics joined with a thin ductile metal layer [١١٥].As the CTE difference between the two ceramics increases, it is noted that the stress intensity factor is governed by the ceramic mismatch and is principally mode II,with only a small mode I component. For small interfacial cracks, K_{II} tends to increase monotonically as the CTE difference between the ceramics becomes large, which results in potentially extensive thermal cracking in the ceramic (based on Fig.٣-٢٣) ,especially when small axial loads are applied which produce a non-zero K_I.

Dreier *et al*.[١١٦] showed a strong dependency of interface fracture behavior on residual thermal stresses under external loading. Notches or performed flaws were produced by grinding a wedge at the interface of a biomaterial specimen fabricated from optical glasses behave linear-elastically, the effect of plasticity in crack propagation is not incorporated. According to their numerical and experimental studies, as $\Delta\alpha$ ($=\alpha_M-\alpha_C$) increases, the increased thermal residual stresses provide a strong mode II contribution at the crack tip, which increases ψ(equation (٣-٢٨)) .The driving force for the crack and kinking angle from the interface were found to increase with ψ. Compared to the effect of residual stresses, the influence of elastic mismatch under external loading on the kinking angle has been shown to be small.

Although experimental results have been obtained with a limited of materials, the results indicate the important effect of residual stresses on interfacial fracture, which makes a crack at the interface tend to deviate away from the interface.

٣.٦.٢ Fracture in the Ceramic

Residual stresses may be obtained from rough estimates by using Equation ٣-٢٧ and the following relationship between defect size and stress level (considering the ceramic side only, and neglecting the contribution from K_{II}:

$$K_I=\pi/٢\ [\sigma(\pi a)^{٠.٥}] \qquad (٣-٢٩)$$

Where K_I is the fracture toughness of ceramics, $\pi/٢$ represents the defect and specimen geometry, σ is the residual stress(no external load applied),and a is the defect size(crack,pore,lack of bonding)[٧].

Fig.٣-٢٢ shows the typical cracking that occurs in the ceramic after cooling from the bonding temperature. The center crack(Fig.٣-٢٢(a)) [١١٣]occurs near the center of the specimen and reflects the principal tensile residual stress in the ceramic near the interface. The perimeter crack in Fig.٣-٢٢-(b) at some distance from the interface depending on the distribution and magnitude of residual stresses in each joint[١١٣-١١٤].

When external stress is imposed on the joint, the fracture of the joint is influenced by the mismatch of elastic properties between the ceramic and the metal, by plastic flow of metal and by the residual

strain caused by the CTE mismatch. In addition, cracking along the interface can occur by the mechanisms in previous section[١١٥].

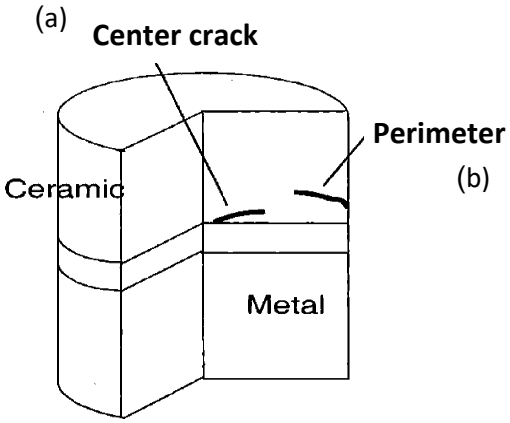

Figure ٣-٢٢: Two most common fracture initiation sites in ceramic-metal joint:

(a)center crack, (b) perimeter crack.[١١٣].